Chapter 7:
Going Nonlinear: Progressing Complexity

May 30, 2011

The early linear stages of structure formation have been succesfully and completely worked out within the context of the linear theory of gravitationally evolving cosmological density and perturbation fields (Peebles 1980). At every cosmologically interesting scale, it aptly and succesfully describes the situation in the early eons after the decoupling of radiation and matter at recombination. It still does so at present on those spatial scales at which the landscape of spatially averaged perturbations resembles a panorama of gently sloping hills. However, linear theoretical predictions soon fail after gravity surpasses its initial moderate impact and nonlinear features start to emerge. Soon thereafter, we start to distinguish the gradual rise of the complex patterns, structures and objects which have shaped our Universe into the fascinating world of astronomy.

Once the evolution is entering a stage in which the first nonlinearities start to mature, it is no longer feasible to decouple the growth of structure on the various involved spatial and mass scales. Rapidly maturing small scale clumps do feel the effect of the large scale environment in which they are embedded. Neighbouring structures not only influence each other by external long-range gravitational forces but also by their impact on resulting matter flows. The morphology and topology of more gradually forming large-scale features will depend to a considerable extent on the characteristics of their content in smaller scale structures that were formed earlier on. This never-ending increasing level of complexity has proved to pose a daunting challenge for developing a fully consistent theoretical framework. No cosmogenic theory as yet has managed to integrate all acquired insights and observed impressions of the world around us.

1. Nonlinear Evolution: Mode Coupling

Once density perturbations become of the order unity, $\delta(\mathbf{x},t) \approx 1$, it is no longer possible to use the basic linear theory of clustering. Different modes of the density fields will start to interact, resulting in mutual "power transfer".

Restricting ourselves to a pure matter-dominated Universe, the full nonlinear fluid evolution equations were (see chapter 4),

$$\boxed{\begin{aligned} \frac{\partial\delta}{\partial t} + \frac{1}{a}\vec{\nabla}_x\cdot(1+\delta)\vec{v} &= 0 \\ \frac{\partial\vec{v}}{\partial t} + \frac{1}{a}\left(\vec{v}\cdot\vec{\nabla}_x\right)\vec{v} + \frac{\dot{a}}{a}\vec{v} &= -\frac{1}{a}\vec{\nabla}_x\phi \\ \nabla_x^2\phi &= 4\pi G\, a^2\,\rho_u\,\delta \end{aligned}} \qquad (1)$$

Rewriting these equations in their corresponding Fourier expressions provides a direct insight into the complications that go along with the growing nonlinearity of a gravitationally evolving system. The Fourier expressions for the density field $\delta(\mathbf{x},t)$, velocity field $\mathbf{v}(\mathbf{x},t)$, and potential field $\phi(\mathbf{x},t$ are

$$\begin{aligned}
\delta(\mathbf{x}) &= \int \frac{d\mathbf{k}}{(2\pi)^3}\,\hat{\delta}(\mathbf{k})\,e^{-i\mathbf{k}\cdot\mathbf{x}} \qquad \Longleftrightarrow \qquad \hat{\delta}(\mathbf{k}) = \int d\mathbf{x}\;\delta(\mathbf{x})\,e^{i\mathbf{k}\cdot\mathbf{x}} \\
\mathbf{v}(\mathbf{x}) &= \int \frac{d\mathbf{k}}{(2\pi)^3}\,\hat{\mathbf{v}}(\mathbf{k})\,e^{-i\mathbf{k}\cdot\mathbf{x}} \qquad \Longleftrightarrow \qquad \hat{\mathbf{v}}(\mathbf{k}) = \int d\mathbf{x}\;\mathbf{v}(\mathbf{x})\,e^{i\mathbf{k}\cdot\mathbf{x}} \\
\phi(\mathbf{x}) &= \int \frac{d\mathbf{k}}{(2\pi)^3}\,\hat{\phi}(\mathbf{k})\,e^{-i\mathbf{k}\cdot\mathbf{x}} \qquad \Longleftrightarrow \qquad \hat{\phi}(\mathbf{k}) = \int d\mathbf{x}\;\phi(\mathbf{x})\,e^{i\mathbf{k}\cdot\mathbf{x}}
\end{aligned} \tag{2}$$

By inserting the Fourier definitions (3) in the fluid equations (2) we find the set of Fourier fluid equations. Formulated in Fourier space, the continuity/energy equation, the Euler equation and the Poisson equation are

$$\begin{aligned}
\frac{d\hat{\delta}(\mathbf{k})}{dt} - \frac{1}{a}\,i\mathbf{k}\cdot\hat{\mathbf{v}}(\mathbf{k}) - \frac{1}{a}\int \frac{d\mathbf{k}'}{(2\pi)^3}\;i\hat{\delta}\,\mathbf{k}'\cdot\hat{\mathbf{v}}(\mathbf{k}-\mathbf{k}') &= 0 \\
\frac{d\hat{\mathbf{v}}(\mathbf{k})}{dt} + \frac{\dot{a}}{a}\,\mathbf{v}(\mathbf{k}) - \frac{1}{a}\int \frac{d\mathbf{k}'}{(2\pi)^3}\;[i\hat{\mathbf{v}}(\mathbf{k}')\cdot(\mathbf{k}-\mathbf{k}')]\;\hat{\mathbf{v}}(\mathbf{k}-\mathbf{k}') &= \frac{1}{a}\,i\mathbf{k}\cdot\hat{\phi}(\mathbf{k}) \\
\frac{\hat{\phi}(\mathbf{k})}{a^2} &= -4\pi G\rho_u\,\frac{\hat{\delta}(\mathbf{k})}{k^2}
\end{aligned} \tag{3}$$

These equations show that in the general nonlinear case the continuity equation and the Euler equation do contain **mode-coupling terms**,

$$\begin{aligned}
&\int \frac{d\mathbf{k}'}{(2\pi)^3}\;i\hat{\delta}\,\mathbf{k}'\cdot\hat{\mathbf{v}}(\mathbf{k}-\mathbf{k}') \qquad \Leftarrow \qquad \text{Continuity equation} \\
&\int \frac{d\mathbf{k}'}{(2\pi)^3}\;\left[i\hat{\mathbf{v}}(\mathbf{k}')\cdot(\mathbf{k}-\mathbf{k}')\right]\;\hat{\mathbf{v}}(\mathbf{k}-\mathbf{k}') \qquad \Leftarrow \qquad \text{Euler equation}
\end{aligned} \tag{4}$$

which will destroy the simple linear situation in which every mode $\mathbf{k}$ would evolve independent of the other modes (see chapter 4). Nonlinear clustering thus manifests itself in the transfer of power between the various scales of the matter distribution.

One may identify many different physical processes that manifest themselves through mode coupling. A straightforward one is the collapse of a peak in the matter density distribution. In the linear regime its spatial configuration remained the same. As soon as an overdensity starts to contract under the influence of its own gravity its structure will be delineated by different scales so that the corresponding modes will start to grow. Also overdense substructures within an overdense region will reach nonlinearity earlier and collapse faster, also an example of crosstalk between different spatial scales. This would involve a top-down process, in which high frequency modes get boosted by the growth of low frequency modes.

It might also be that the evolution of large sized features will get affected by its substructure, it would not be inconceivable for the evolution of large objects to be seriously affected by the earlier collapse and formation of its internal structure. This is a bottom-up process in which high frequency modes affect the evolution of low frequency modes. Indeed, if the latter were significant it would pose a tremendous challenge to the theory of structure formation. One would need to take into account the internal evolution and structure of an object. It would render useless the conventional methodology of filtering out high frequency modes and analyzing the subsequent structure in terms of linear theory. One may prove that is not a serious problem as long as the power spectrum $P(k)$ of fluctuations is not steep enough (see Peebles 1980):

$$n(k) \,=\, \frac{d\log P(k)}{d\log k} \,<\, 4\,. \tag{5}$$

2. Nonlinear Clustering Descriptions

Lacking useful symmeteries, the study of structure formation has furnished an abundance of mutually complementary descriptions. Each focuses on one or more particular aspects, sometimes isolating those deemed relevant at the cost of neglecting others. Our ideas of the workings of the gravitational instability process have therefore progressed and been shaped by a wide range of different theoretical and numerical approaches and techniques. In terms of methodology we may therefore identify and discern several different attitudes. In this section we will provide an overview of a few of the most used techniques for studying nonlinear clustering. Subsequently, we will first work out the Zel'dovich approximation before discussing its wider context of the Lagrangian description of structure formation.

2.1. Eulerian Perturbation Theory

The most straightforward approach towards extending the linear description of structure formation is that of pursuing the Eulerian view of describing the evolution of a physical system. Seeking to expand the fluid equations beyond the linear regime towards higher order terms has produced some impressive advances.

It has produced a huge complex of advanced and complicated nonlinear perturbation analyses (for an extensive review, see Bernardeau et al. 2002). In particular the third order and additional lower order perturbation terms have have proven to be particularly apt in uncovering and highlighting important statistical clues and signatures. In this, Eulerian perturbation theory has been at the basis of defining essential tools for discriminating between viable formation scenarios.

However, it has been less helpful in guiding our physical intuition concerning the unfolding of the complex patterns we see forming in the more advanced phases of structure formation. Also, while beyond the linear regime any incremental step in the order of the perturbation involves an overpowering expansion in mathematical complexity it has the adversery of being a relevant correction only during an ever decreasing dynamical timespan. Due to the acceleration of the gravitational instability process the corresponding timescales also decrease correspondingly. Eulerian perturbation theory therefore quickly involves an almost unsurmountable amount of effort.

2.2. Lagrangian Perturbation Theory

A closely affiliated approach to Eulerian perturbation theory is a similar perturbation analysis following the Lagrangian description of the system. **Lagrangian** approaches have proven to be the most fruitful approach in developing a physical intuition of the structural evolution during the more advanced stages. By following the matter elements on their path through the evolving cosmic matter field it is easier to appreciate the various forces and deformation tendencies acting on them. It is in particular the formulation of the first-order **Zel'dovich approximation** (Zel'dovich 1970) which has been of eminent importance in the study of cosmological structure formation. First and foremost, it did elucidate and explain qualitatively the basic tendencies of gravitational contraction in an evolving cosmos, in particular the tendency to do so anisotropically. In addition to its conceptual significance, it assumed extensive influence by providing computational cosmologists with the machinery to set up the initial conditions of cosmological N-body simulations for a wide variety of structure formation scenarios.

2.3. Simplified Configurations

Another approach is trying to follow the full nonlinear evolution in a few conceptually simple configurations. Such configurations would emphasize particular physical mechanisms and processes. By isolating these and studying their impact one may better understand their possible imprint in the more complex world of reality. Such configurations usually figure as templates for interpreting the observational world or of the outcome of computer simulations. By far the most important examples is that of the **Spherical Model**. Another useful model is that of the **Homogeneous Ellipsoidal Model**, which has been of benefit in obtaining substantial insight into the mechanisms and characteristics of anisotropic pattern formation.

2.4. General Pattern Configurations

One approach seeks to formulate approximate descriptions of the full matter distribution, valid during either a restricted cosmic period or in the case of a few particular scenarios. Such descriptions should be able to provide an approximate description of clustering in a generic random density and velocity field.

The prime example, crucial for the study of cosmic structure formation, is the **Zel'dovich approximation**. In fact, while this description proved to be an extremely useful and important approximation of clustering in the mildly nonlinear regime, i.e. $\delta \approx$ few, formally it involves the conceptually important theory of linear Lagrangian perturbation theory.

2.5. N-body simulations

The translation of self-gravitating systems into N-body computer simulations may be considered to be the the visibly most appealing and informative approach for studying the formation of structure in the Universe. The use of N-body computer models and calculations to simulate the evolution of cosmic structure through the force of gravity is undoubtedly the most widely known and exploited Lagrangian formulation for studying cosmic structure formation.

N-body simulations are unique in their ability to deal with the entire evolution of a system through the full range of linear up to highly nonlinear stages. In principal N-body simulations are suited for any feasible configuration, independent of structural complexities and lack of helpful symmetries. Equally important is that the N-body approach is not principally restricted to purely gravitationally evolving systems. As evidenced by an array of computer codes developed over the past decade, it is rather straightforward to incorporate the influence and workings of a range of complicating (often dissipational) physical effects and processes. Sophisticated computer codes have been able to succesfully incorporate gravity, gasdynamical processes, atomic processes and a range of other complicating factors into codes simulating the formation and evolution of cosmic structures.

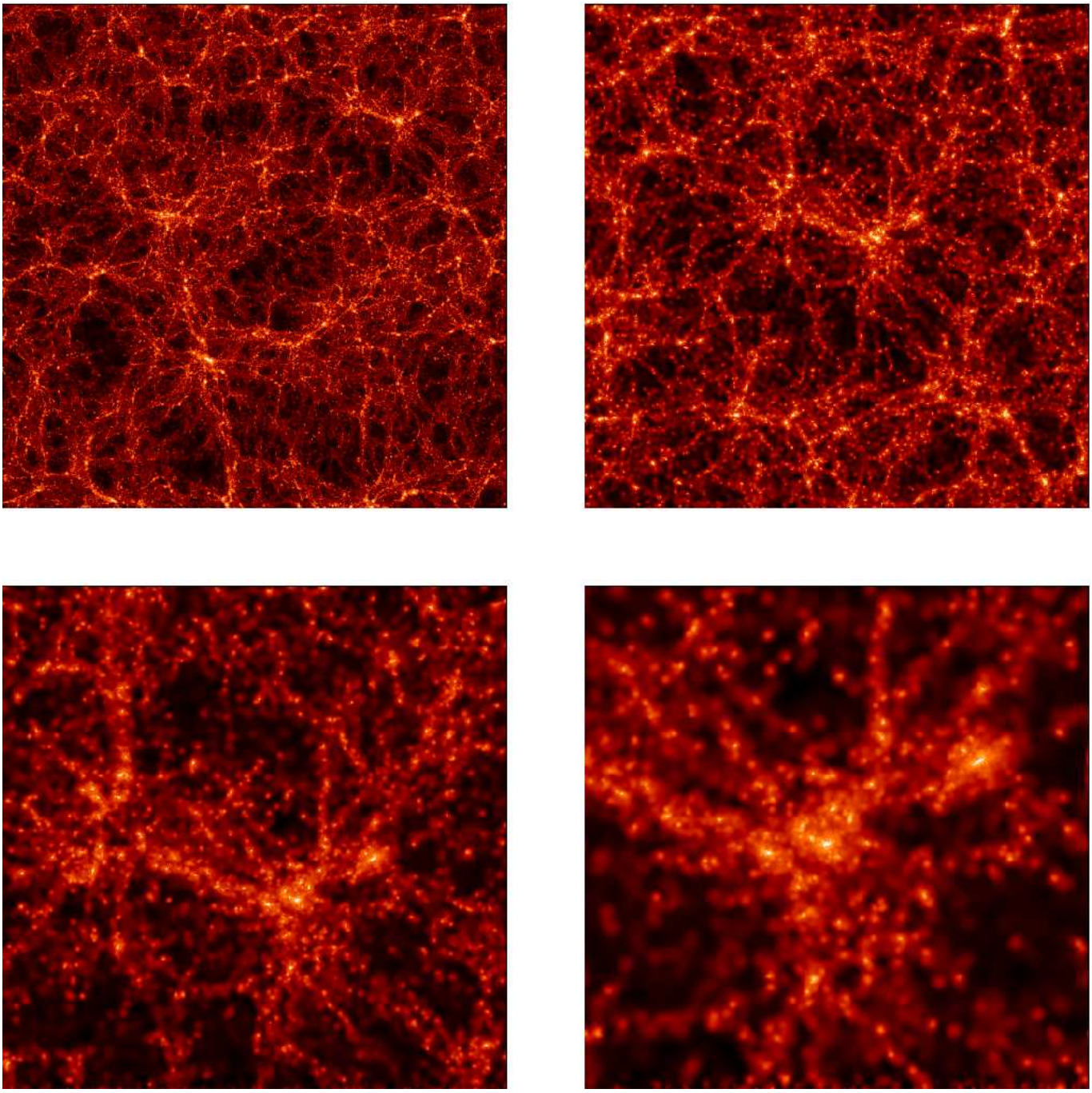

Figure 1. A mosaic of 4 blow-ups from a 256^3 particle simulation by the Virgo consortium, corresponding to a SCDM scenario mass distribution at $z = 0$. Courtesy: VIRGO/Colberg et al.

However, the success and visual appeal of N-body simulations often also lead to overinterpretation. Many scientific studies unjustifiably ignore the limitations and artefacts of the computer calculations. Even the word "simulation" already carries with it the pretention of the computer models representing reality. It would be more honest, as well as modest, to talk about "computer experiments". Also, an attitude has developed in which the reproduction of observed patterns or results by a computer model is considered to be an explanation in itself. This is far from true, the computer models should be used as mere guidelines. A true physical understanding may at best only start or be guided by computer experiments.

3. Lagrangian Perturbation Theory

In the Eulerian approach we describe the evolution of a system at a fixed location. The change in the physical state of a system at a particular location is the result of two factors. First there are the intrinsic local changes of the system. Secondly, the system changes locally as a result of the energy flows in the system, i.e. as a result of energy flowing in and out of the local volume. The alternative approach to describing the physical evolution of the system is to follow the matter (energy) elements on their path through the evolving cosmic matter field. This allows an easier appreciation of the various forces and deformation tendencies acting on the volume elements. By studying the evolution of a system on the basis of the basic Lagrangian fluid equations the character of various tendencies in the evolution of the matter distribution are easier to understand.

Mathematically, the conversion involves a transformation from an Eulerian to a Lagrangian time derivative. The conversion in spatial coordinates $\mathbf{r}$ proceeds as

$$\boxed{\frac{d}{dt} \equiv \frac{\partial}{\partial t} + \mathbf{u}\cdot\nabla\ ,} \tag{6}$$

where $\mathbf{u}$ is the velocity of the moving fluid element. In chapter 4 we have already seen that the Euler equation is the Lagrangian formulation of Newton's second law. In physical coordinates the Lagrangian Euler equation then simply means

$$\frac{d\mathbf{u}}{dt} = -\nabla_{\mathbf{r}}\Phi\,. \tag{7}$$

For the comoving coordinate system $\mathbf{x}$, the Lagrangian time derivative is likewise defined by the transformation

$$\boxed{\frac{d}{dt} \equiv \frac{\partial}{\partial t} + \frac{1}{a}\mathbf{v}\cdot\nabla\ ,} \tag{8}$$

with $\mathbf{v}$ the peculiar velocity of the fluid element. The Euler equation in comoving coordinates may then be expressed as

$$\frac{da\mathbf{v}}{dt} = -\frac{1}{a}\nabla\phi\,. \tag{9}$$

with the ∇ operator defined for comoving coordinates $\mathbf{x}$, i.e. ∇_x.

3.1. Evolution and Deformation: Lagrangian View

As a given patch of matter participates in the evolution of the matter distribution it will evolve. In its totality it will flow along a path defined by the forces it experiences. Its density will change as it gets *compressed* or as it *expands*. Shearing flows, in a gravitational system the result of tidal forces, will deform the shape of the patch.

In the Lagrangian formulation the description of the deformation of a given fluid element is of central importance. It is straightforward to see that the deformations are closely linked to the flow field in and around the fluid element. The various components of the deformation of the evolving mass element at comoving location $\mathbf{x}$ are therefore encoded in the decomposition of the gradient of its velocity field $\mathbf{v}$ (the rate-of-strain tensor).

3.1.1. Expansion, Vorticity and Shear

We can distinguish three different modes, the **expansion/compression** θ, the **shear** σ_{ij} and the **vorticity** tensor elements ω_{ij}, which contribute to the velocity deformation tensor $v_{i,j}$ as

$$\boxed{\frac{1}{a}\frac{\partial v_i}{\partial x_j} \;=\; \frac{1}{3}\theta\,\delta_{ij} \;+\; \sigma_{ij} \;+\; \omega_{ij}\;,} \tag{10}$$

in which the expansion θ is the trace of the velocity field gradient, $\sigma_{ij} = \sigma_{ji}$ the traceless symmetric part and $\omega_{ij} = -\omega_{ji}$ the antisymmetric part (and ϵ_{ijk} the Levi-Civita symbol),

$$\boxed{\begin{aligned} \theta \;=\; \frac{1}{a}\nabla\cdot\mathbf{v} \quad &\equiv \quad \frac{1}{a}\left(\frac{\partial v_1}{\partial x_1}+\frac{\partial v_2}{\partial x_2}+\frac{\partial v_3}{\partial x_3}\right) \\ \sigma_{ij} \quad &\equiv \quad \frac{1}{2a}\left(\frac{\partial v_i}{\partial x_j}+\frac{\partial v_j}{\partial x_i}\right)-\frac{1}{3}(\nabla\cdot\mathbf{v})\,\delta_{ij} \\ \omega_{ij} \quad &\equiv \quad \frac{1}{2a}\left(\frac{\partial v_i}{\partial x_j}-\frac{\partial v_j}{\partial x_i}\right) \end{aligned}} \tag{11}$$

The vorticity tensor ω_{ij} is related to the vorticity $\vec{\omega}$ of the fluid through the relations

$$\begin{aligned} \omega_{ij} \quad &= \epsilon_{ijk}\omega^k \\ \vec{\omega} \quad &= \quad \frac{1}{2a}\nabla\times\mathbf{v} \end{aligned} \tag{12}$$

with ϵ_{ijk} the three-dimensional Levi-Civita symbol. Notice that we transformed from physical coordinates $\mathbf{r}$ to comoving coordinates $\mathbf{x}$, and from the full velocity $\mathbf{u}$ to the peculiar velocity $\mathbf{v}$. This we can easily do as the global Hubble expansion is a pure expansion (or compression) flow, only and exclusively involving a global velocity divergence Θ_H,

$$\Theta_H \;=\; 3\,H(t) \tag{13}$$

so that we may easily transform to the comoving velocity deformation quantities by subtracting Θ_H from the full velocity divergence Θ,

$$\Theta \,=\, \theta \,+\, 3H(t)\,. \tag{14}$$

These quantities describe the change of a mass element during the evolution of a system. The *expansion term* θ describes its expansion or contraction. It is the one component responsible for the change in density (see next subsection). The shear tensor σ_{ij} describes the change in shape of the matter element. By diagonalizing the shear tensor matrix σ_{ij} we can infer the principal axes for the shape change from the direction of the eigenvectors while the eigenvalues describe the strength of this shape deformation along each of the principal axes. The last factor of change that may affect the fluid element is rotations due to the presence of a vorticity term, ω_{ij}.

3.1.2. Lagrangian fluid equations

With the tools to describe the changing volume of the mass element whose evolution is followed by the Lagrangian description, we can infer the equations that describe its evolution. The formalism which we will present here is based on two implicit restrictions. First, we will assume pure laminar flow and follow fluid elements as long as they have not crossed the paths of other fluid elements. This allows us to limit outselves to a pure local description by focussing on the evolution of individual fluid elements. Secondly, we will restrict ourselves to a pressureless, purely gravitational system and ignore the influence of pressure forces.

In the Eulerian formalism we described the evolution of the system in terms of comoving space, and within the same context of density and velocity perturbations against the background of an expanding Universe we follow the same strategy to unfold a Lagrangian description of the evolving perturbations.

While the Eulerian description is focussing on the local change of perturbation quantities, and deals with a constant (infinitesimal) volume element at a fixed (comoving) location $\mathbf{x}$ the Lagrangian description has the additional need to describe the deformation of a particular volume element. Its volume will change as it expands or contracts. Meanwhile generically also its shape and orientation will change while flowing along space. It will therefore not be sufficient to just describe the change of the density excess or deficit δ, the accompanying peculiar velocity and gravitational potential. A proper and complete description will have to address the development of the expansion/contraction θ, shear σ_{ij} and rotation ω_{ij} of the fluid element. These deforming tendencies will in turn affect density, velocity and potential. A complete Lagrangian formulation should therefore consist of more equations than the Eulerian set of equations.

In total there are seven equations. One equation concerns the definition of the peculiar velocity $\mathbf{v}$ of the fluid element. Subsequently we have the Lagrangian equivalents of the three Eulerian fluid equations, the continuity equation for ensuring mass conservation, Newton's second law as the Lagrangian equivalent of the Euler equation and the Poisson equation. In addition we need to account for the evolution of the expansion/contraction θ, which in turn is affected by the shear σ_{ij} and vorticity ω_{ij}. For a full characterization one therefore also needs the equations for the evolution of the shear and vorticity.

The first equation is rather straightforward and merely involves the definition of the peculiar velocity $\mathbf{v}(\mathbf{x}, t)$,

$$\boxed{\mathbf{v} \,\equiv\, a\,\frac{d\mathbf{x}}{dt} \,=\, \frac{d\mathbf{x}}{d\tau}\,.} \tag{15}$$

in which the conformal time τ,

$$d\tau \,=\, \frac{dt}{a} \tag{16}$$

is used as the time derivative in the right expression. The first evolution equation to consider is the Lagrangian **continuity/energy** equation, expressing the conservation of mass/energy of the fluid element. A change in density is a result of the expansion or contraction of the volume of the fluid element. While the Eulerian description looks at a fixed volume element and has to take account of the inflowing and outflowing flux of energy, the Lagrangian view is that of a fluid element of a fixed mass/energy content and changing density contrast δ as the result of the expansion/contraction θ of its volume,

$$\boxed{\frac{d\delta}{dt} \; + \; a\,(1+\delta)\;\theta \;=\; 0} \tag{17}$$

The equation of motion of the fluid element – the Euler equation – can be directly inferred from its Eulerian version,

$$\frac{\partial \mathbf{v}}{\partial t} \; + \; \frac{1}{a}\;(\mathbf{v}\cdot\nabla)\;\mathbf{v} \; + \; \frac{\dot{a}}{a}\,\mathbf{v} \quad = \quad -\frac{1}{a}\,\nabla\phi \tag{18}$$

and the expression for the translation from a **comoving Eulerian** to a **comoving Lagrangian formulation**, eqn. (8),

$$\boxed{\frac{d\mathbf{v}}{dt} \;=\; -\,\frac{\dot{a}}{a}\,\mathbf{v} \;-\; \frac{1}{a}\,\nabla\phi}$$

In a more compact and direct notation this becomes

$$\frac{da\mathbf{v}}{dt} \;=\; \nabla\phi\,. \tag{19}$$

from which we can directly infer that in the absence of a source potential ϕ the peculiar velocity $\mathbf{v}$ of the fluid element rapidly decays away,

$$\mathbf{v} \;\propto\; \frac{1}{a}\,. \tag{20}$$

A similar conclusion had already been found for the peculiar velocity in the linear regime, for the strictly Eulerian case. For linking the force sourceterm – the potential ϕ – to the matter distribution the expression in the Lagrangian formalism is the same as that for the Eulerian formalism. In other words, we retain the same **Poisson Equation**,

$$\boxed{\nabla^2\phi \;=\; 4\pi G\,a^2\,\rho_u\,\delta} \tag{21}$$

Upon assessing the above set of three Lagrangian fluid equations, we find that they include the explicit velocity divergence term θ, the trace of $\nabla_i v_j$. While one might evaluate θ by explicitly solving for $\mathbf{v}$, a better approach is to use an explicit expression for the evolution of θ. This is the **Raychaudhury equation**,

$$\boxed{\frac{d\theta}{dt} \;+\; 2\,\frac{\dot{a}}{a}\,\theta + \frac{1}{3}\,\theta^2 \;+\; \sigma^{ij}\sigma_{ij} \;-\; 2\vec{\omega}^2 \;=\; -4\pi G\rho_u\delta} \tag{22}$$

The Raychaudhury equation follows from an evaluation of the Euler fluid equation (19) in combination with the Poisson equation (21).

The Raychaudhury equation introduces an interesting new element to our evaluations of an evolving matter distribution. Through the quadratic **shear term** $\sigma^{ij}\sigma_{ij}$ and the quadratic **vorticity term** $2\vec{\omega}^2 = \omega^{ij}\omega_{ij}$ it includes an explicit term for the influence of shear on the evolution of fluid elements. Two observations may be made immediately. First, the shear and vorticity term appear to act like a source term, be it with opposite signs. The presence of shear accelerates the evolution of mass elements: while

$$\frac{d\theta}{dt} \propto -\sigma^{ij}\sigma_{ij}\,, \tag{23}$$

any presence of shear translates into an increase of the compression of a fluid element as θ tends to turn more negative. The reverse influence is that of vorticity. Because

$$\frac{d\theta}{dt} \propto \vec{\omega}^2\,, \tag{24}$$

the presence of vorticity will oppose any collapsing tendency and instead tend to promote the expansion of a fluid element. Secondly, the influence of shear and vorticity is propragated via a quadratic terms, which means that they it involves pure **nonlinear effects**. During the linear regime the influence of shear and vorticity is negligible. It had indeed not been observed to play a significant, modifying, influence in the treatment of linear structure evolution.

With the introduction of the shear and vorticity term as significant evolutionary influences we will also have to consider their evolution in order to formulate a **closed**, complete, system of equations for the evolution of the mass distribution.

The **Lagrangian Vorticity equation** describes the evolution of the vorticity $\vec{\omega}$ of a fluid element. It follows from an evaluation of the antisymmetric part of the Euler equation, in combination with the continuity equation.

$$\boxed{\frac{d\omega^i}{dt} + 2\,\frac{\dot{a}}{a}\,\omega^i + \frac{2}{3}\,\theta\,\omega^i - \sigma_{ij}\,\omega^j = 0} \tag{25}$$

This expression shows that if there is no primordial vorticity, i.e. if $\vec{\omega} = 0$, then the flow remains vorticity free. This confirms the earlier assessment in the linear regime. This of course remains valid up to the limitation of the Lagrangian description presented here. When flows are no longer laminar and start to cross the situation gets more complex and vorticity may be generated.

For the evolution of the shear σ_{ij} the **Lagrangian Shear equation** can be derived from the symmetric part of the Euler equation, in combination with the continuity equation,

$$\boxed{\frac{d\sigma_{ij}}{dt} + 2\,\frac{\dot{a}}{a}\,\sigma_{ij} + \frac{2}{3}\,\theta\,\sigma_{ij} + \sigma_{ik}\,\sigma^k_j - \frac{1}{3}\delta_{ij}\,(\sigma^{kl}\sigma_{kl}) = -T_{ij}} \tag{26}$$

where T_{ij} is the gravitational tidal field working on the fluid element,

$$T_{ij}(\mathbf{x}) = \frac{1}{a^2}\left\{\frac{\partial^2\phi}{\partial x_i \partial x_j} - \frac{1}{3}\nabla^2\phi\;\delta_{ij}\right\}\,. \tag{27}$$

Within the context of general relativity T_{ij} is the electric part of the Weyl tensor in the fluid frame. As expected this equation is an expression of how the gravitational tidal field acts as a source term for inducing a shear component in the flow field. To be able to evaluate the value of T_{ij} we need the Poisson equation for computing the gravitational potential field.

3.1.3. Irrotational flow

In our discussion of the linear regime we had noticed that in the case of a pressureless, purely gravitationally evolving system primordial vorticity will decay during linear evolution. This conclusion may be extrapolated towards the nonlinear regime. The **Lagrangian vorticity equation** (25) shows that if a primordial fluid element is irrotational it will remain so during its further nonlinear evolution (up to streamlines crossing).

Under the assumption that the fluid is pressureless and irrotational (i.e. $\omega_i = 0$), the evolution of a fluid element – with comoving trajectory $\mathbf{x}(t)$ – is specified by six first order differential equations. In summary, the complete set of irrotational Lagrangian fluid equations is:

$$
\begin{aligned}
\mathbf{v} &= a\,\frac{d\mathbf{x}}{dt} \\
\frac{d\mathbf{v}}{dt} + \frac{\dot{a}}{a}\,\mathbf{v} &= -\frac{1}{a}\,\nabla\phi \\
\frac{d\delta}{dt} + (1+\delta)\,\theta &= 0 \\
\frac{d\theta}{dt} + 2\,\frac{\dot{a}}{a}\,\theta + \frac{1}{3}\,\theta^2 + \sigma^{ij}\sigma_{ij} &= -4\pi G\rho_u\delta \\
\frac{d\sigma_{ij}}{dt} + \frac{\dot{a}}{a}\sigma_{ij} + \frac{2}{3}\,\theta\,\sigma_{ij} + \sigma_{ik}\,\sigma^k_j - \frac{1}{3}\delta_{ij}\,(\sigma^{kl}\sigma_{kl}) &= -T_{ij} \\
\nabla^2_x\phi &= 4\pi G\,a^2\,\rho_u\,\delta \\
T_{ij}(\mathbf{x}) &= \frac{1}{a^2}\left\{\frac{\partial^2\phi}{\partial x_i\partial x_j} - \frac{1}{3}\nabla^2\phi\;\delta_{ij}\right\}
\end{aligned}
\tag{28}
$$

3.1.4. Lagrangian collapse

An interesting observation follows from evaluating the combination of the continuity and Raychaudhuri equation. It leads to a second order ordinary differential equation describing the evolution of the density contrast δ of a fluid element:

$$
\frac{d^2\delta}{dt^2} + 2\,\frac{\dot{a}}{a}\,\frac{d\delta}{dt} = \frac{4}{3}(1+\delta)^{-1}\left(\frac{d\delta}{dt}\right)^2 + (1+\delta)\left(\frac{2}{3}\sigma_{ij}\sigma_{ij} - 2\vec{\omega}^2 + 4\pi G\rho_u\delta\right)
\tag{29}
$$

Bertschinger & Jain (1994) noted that this equation shows that in the absence of vorticity the presence of a nonzero shear increases the rate of growth of density fluctuations (vorticity will inhibit this process). In other words, the rate of growth of δ gets amplified in the presence of shear. This conclusion holds independently of assumptions about the evolution of shear or tides and is due to the simple geometrical fact that shear increases the rate of growth of the convergence ($\propto -\theta$) of fluid streamlines.

With zero shear and vorticity the velocity gradient tensor is isotropic, corresponding to uniform spherical collapse with radial motions towards some centre (see sect. (**??**). Equation (29) then reduces to the exact equation for the evolution of the mean density in the spherical model,

$$\frac{d^2\delta}{dt^2} + 2\,\frac{\dot{a}}{a}\,\frac{d\delta}{dt} = \frac{4}{3}(1+\delta)^{-1}\left(\frac{d\delta}{dt}\right)^2 + 4\pi G\rho_u\delta(1+\delta) \tag{30}$$

An important and immediate observation is that this implies the growth of uniform spherical perturbations to be more slowly than more generic anisotropic configurations with a nonzero shear term:

Shear streaming accelerates Collapse:

$\Longleftrightarrow$

Spherical Collapse is slowest !!!

EXERCISE: Derive expression (30) for the evolution of the density $\delta(r,t)$ of a shell in the spherical model. Note: use the equations for the spherical model in section (5).

3.1.5. Localized Lagrangian Approximations

Careful consideration of the first three fluid equations shows that the Lagrangian description entails a nearly exclusive **local** view of the evolution of the matter distribution. All quantities relate to the "local" values pertaining to one particular piece of matter.

The one remaining complication for transforming the Lagrangian fluid equations into such *local* descriptions involves the development of the driving shear term σ_{ij}. Evidently, its evolution depends on the behaviour of the gravitational tide T_{ij}. Obviously, its value is generically determined by the full matter distribution throughout the cosmic volume. Ultimately, the one non-local ingredient is that of the gravitational field, involving contributions from all over space. There have been various attempts to circumvent these *non-local* complications by developing approximate schemes for the evolution of the gravitational field.

The *locality* of these approximation schemes implies the evolution to be described by a set of *ordinary differential equations* for each mass element, with no coupling to other mass elements aside from those implied by the initial conditions. Note that N-body simulations are distinctly *non-local* Lagrangian descriptions. At every timestep the full gravitational potential set by the full cosmic matter distribution needs to be evaluated at the location of every mass element.

We will see that the Zel'dovich approximation (1970) is the most succesfull representative of a class of Lagrangian approximation schemes in which the nonlinear dynamics of selfgravitating matter is encapsulated into an approximate "local" formulation (Bertschinger & Jain 1994, Hui & Bertschinger 1996). In these localized Lagrangian approaches, the density, velocity gradient, and gravity gradient for each mass element behaves as if the element evolves independently of all the others once the initial conditions are specified. For instance, the evolution of a given mass element under the Zel'dovich approximation is completely determined once the initial expansion, vorticity, shear and density at this

mass element are specified. The influence of other mass elements on the subsequent evolution of these quantities at this particular mass element is then assumed to be *fully encoded in the initial conditions*, and unaffected by the subsequent evolution of these other mass elements. Such a presumption may seem implausible in view of the unrestrained long-range gravitational force, yielding a noticeable influence from all other mass elements in the Universe.

Yet, the success of the Zel'dovich approximation, having provided a great deal of insight into the essentials of nonlinear evolution of density fluctuations, demonstrates how useful such schemes in fact can be.

4. Zel'dovich Approximation

By means of a Lagrangian perturbation analysis Zel'dovich (1970) proved, in a seminal contribution, that to first order – typifying early evolutionary phases – the reaction of cosmic patches of matter to the corresponding peculiar gravity field would be surprisingly simple. The resulting expression involves a plain ballistic linear displacement set solely by the initial (Lagrangian) force field. It frames the well-known **Zel'dovich approximation**.

The essence of the Lagrangian formalism is a mapping from the initial comoving position $\mathbf{q}$ of a mass element onto its location $\mathbf{x}(\mathbf{q}, t)$:

$$\boxed{\mathbf{q} \quad \longrightarrow \quad \mathbf{x}(\mathbf{q}, t)} \tag{31}$$

The initial comoving location $\mathbf{q}$ is the Lagrangian coordinate of the matter element, and will be used as a "tag" to identify it while moving along its path $\mathbf{x}(\mathbf{q})$. Of course the Lagrangian coordinate of each mass element remains the same throughout cosmic time. The Lagrangian perturbation formalism describes the displacement

$$\mathbf{s} \equiv \mathbf{x} - \mathbf{q} \tag{32}$$

of a mass element in terms of an ordered sequence of moments of displacement,

$$\mathbf{x}(\mathbf{q}, t) \;=\; \mathbf{q} \;+\; \mathbf{x}^{(1)}(\mathbf{q}, t) \;+\; \mathbf{x}^{(2)}(\mathbf{q}, t) \;+\; \ldots \tag{33}$$

in which the successive terms $\mathbf{x}^m$ correspond to successive terms of the relative displacement $|\partial(\mathbf{x} - \mathbf{q})/\partial\mathbf{q}|$,

$$1 \gg \left|\frac{\partial \mathbf{x}^{(1)}}{\partial \mathbf{q}}\right| \gg \left|\frac{\partial \mathbf{x}^{(2)}}{\partial \mathbf{q}}\right| \gg \left|\frac{\partial \mathbf{x}^{(3)}}{\partial \mathbf{q}}\right| \gg \ldots \tag{34}$$

The Zel'dovich approximation is the solution of the Lagrangian fluid equations for small density perturbations ($\delta^2 \ll 1$), corresponding to a solution for its displacement $\mathbf{s}$ truncated at the first order $\mathbf{x}^{(1)}$ in the above Lagrangian perturbation series. The Zel'dovich approximation thus corresponds to a simple linear prescription for the displacement of a particle.

4.0.6. Zel'dovich Mapping and Density Evolution

Given the mapping from the Lagrangian coordinate $\mathbf{q}$ to the Eulerian coordinate $\mathbf{x}$, we may infer the **density evolution** induced by the displacement of the mass by the demand of **mass conservation**. The mass originally contained in an infinitesimal volume $d\mathbf{q}$ is transported to the infinitesimal volume $d\mathbf{x}$. The density in Lagrangian space $\mathbf{q}$ is of course equal to the average cosmic density at time t, $\rho_u(t)$. On the basis of mass conservation within we then find that the density at position $\mathbf{x}$ in Eulerian space is

$$\rho(\mathbf{x}, t)\, d\mathbf{x} \;=\; \rho_u(t)\, d\mathbf{q} \tag{35}$$

so that we find that the density perturbation $\delta(\mathbf{x}, t)$ is

$$\boxed{1 \,+\, \delta(\mathbf{x}, t) \;=\; \frac{\rho(\mathbf{x}, t)}{\rho_u(t)} \;=\; \left\| \frac{\partial \mathbf{x}}{\partial \mathbf{q}} \right\|^{-1}} \tag{36}$$

with $\| \cdots \|$ the Jacobian determinant.

4.0.7. Lagrangian Perturbation theory

To compute the Jacobian determinant 36) in terms of the Lagrangian perturbation series, we take the Jacobian from the expression (33) for the displacement $(\mathbf{x} - \mathbf{q})$,

$$\begin{aligned} \frac{\partial \mathbf{x}}{\partial \mathbf{q}} \;&=\; \mathbb{1} + \frac{\partial \mathbf{x}^{(1)}}{\partial \mathbf{q}} + \frac{\partial \mathbf{x}^{(2)}}{\partial \mathbf{q}} + \cdots \\ &\approx \begin{pmatrix} 1 + \frac{\partial x_1^{(1)}}{\partial q_1} & \frac{\partial x_2^{(1)}}{\partial q_1} & \frac{\partial x_3^{(1)}}{\partial q_1} \\ \frac{\partial x_1^{(1)}}{\partial q_2} & 1 + \frac{\partial x_2^{(1)}}{\partial q_2} & \frac{\partial x_3^{(1)}}{\partial q_2} \\ \frac{\partial x_1^{(1)}}{\partial q_3} & \frac{\partial x_2^{(1)}}{\partial q_3} & 1 + \frac{\partial x_3^{(1)}}{\partial q_3} \end{pmatrix} \end{aligned} \tag{37}$$

In this $\mathbb{1}$ is the identity matrix. To first order the Jacobian determinant can therefore be written as

$$\left\| \frac{\partial \mathbf{x}}{\partial \mathbf{q}} \right\| \;\approx\; \left(1 + \frac{\partial x_1^{(1)}}{\partial q_1}\right) \left(1 + \frac{\partial x_2^{(1)}}{\partial q_2}\right) \left(1 + \frac{\partial x_3^{(1)}}{\partial q_3}\right) + \cdots \tag{38}$$

$$\approx\; 1 \,+\, \nabla_{\mathbf{q}} \cdot \mathbf{x}^{(1)} \,+\, \mathcal{O}(\cdots) \tag{39}$$

Using this result we then obtain the first order approximation for the density perturbation, $\delta^{(1)}(\mathbf{x}, t)$, by inserting the first order expression for the Jacobian matrix in eqn. (36),

$$\boxed{\delta^{(1)}(\mathbf{x}, t) \;=\; -\nabla_{\mathbf{q}} \cdot \mathbf{x}^{(1)}} \tag{40}$$

This relation between density perturbation $\delta^{(1)}$ and displacement $\mathbf{x}^{(1)}$ allows us to infer a relation between the primordial potential perturbation $\phi^{(1)}$ and $\mathbf{x}^{(1)}$ via the Poisson equation,

$$\nabla^2 \phi^{(1)} \;=\; 4\pi G\, \rho_u\, a^2\, \delta^{(1)} \;=\; -4\,\pi G\, \rho_u\, a^2\, \nabla_{\mathbf{q}} \cdot \mathbf{x}^{(1)}\,. \tag{41}$$

If we restrict the analysis to the **longitudinal part** $\mathbf{x}_{\parallel}^{(1)}$ of the displacement and assume that the transversal component $\mathbf{x}_{\perp} = 0$,

$$\mathbf{x}^{(1)} \quad = \quad \mathbf{x}_{\parallel}^{(1)} + \mathbf{x}_{\perp}^{(1)}$$

$$\nabla_{\mathbf{q}} \times \mathbf{x}_{\parallel}^{(1)} \, = \, 0 \quad \Longleftarrow \quad \mathbf{x}_{\parallel}^{(1)} \, = \, \nabla\chi \tag{42}$$

$$\nabla_{\mathbf{q}} \cdot \mathbf{x}_{\perp}^{(1)} \, = \, 0 \quad \Longleftarrow \quad \mathbf{x}_{\perp}^{(1)} \, = \, \nabla \times \mathbf{A} \tag{43}$$

we may invert the Poisson equation to yield

$$\nabla\phi^{(1)} \, = \, -\, 4\pi G\, \rho_u\, a^2\, \mathbf{x}^{(1)} \, . \tag{44}$$

Inserting this expression in the Euler equation corresponding to the first order displacement $\mathbf{x}^{(1)}$,

$$\frac{d\mathbf{v}^{(1)}}{dt} \, + \, \frac{\dot{a}}{a}\, \mathbf{v}^{(1)} \quad = \quad -\frac{1}{a}\, \nabla\phi^{(1)} \tag{45}$$

$$\mathbf{v}^{(1)} \, = \, a\, \frac{d\mathbf{x}^{(1)}}{dt}$$

we find the equation for the evolution for $\mathbf{x}^{(1)}$ is given by the familiar second order ordinary differential equation

$$\boxed{\frac{d^2\mathbf{x}^{(1)}}{dt^2} \, + \, 2\frac{\dot{a}}{a}\, \frac{d\mathbf{x}^{(1)}}{dt} \, = \, 4\pi\, G\rho_u\, \mathbf{x}^{(1)}} \tag{46}$$

The firs order displacement $\mathbf{x}^{(1)}\mathbf{q}, t)$ is therefore described by the same differential equation as that of the density perturbations δ in the linear regime. We thus find that the displacement $\mathbf{x}^{(1)}$ may be written in terms of a growing mode solution and a decaying mode solution,

$$\mathbf{x} - \mathbf{q} \, = \, D_+(t)\, \vec{\psi}_+(\mathbf{q}) \, + \, D_-(t)\, \vec{\psi}_-(\mathbf{q}) \tag{47}$$

in which the growth factors $D_+(t)$ and $D_-(t)$ are the same as the linear density growth factors extensively treated in chapter 4. Because we have restricted the analysis to the longitudinal solution relevant to gravitational instability the vector fields ψ are also longitudinal,

$$\nabla \times \vec{\psi} \, = \, 0 \quad \Longrightarrow \quad \vec{\psi} \, = \, -\vec{\nabla}\Psi(\mathbf{q}) \tag{48}$$

in which we have written the field ψ as the gradient of the "displacement potential" field Ψ. Discarding the decaying solution this brings us to the ultimate expression embodying the **Zel'dovich formalism**,

$$\boxed{\mathbf{x} \, = \, \mathbf{q} \, - \, D(t)\, \vec{\nabla}\Psi(\mathbf{q})} \tag{49}$$

or, in terms of the displacement vector $\psi(\mathbf{q})$,

$$\boxed{\mathbf{x} \, = \, \mathbf{q} \, + \, D(t)\, \vec{\psi}(\mathbf{q})} \tag{50}$$

4.0.8. Zel'dovich formalism: Peculiar Velocity

From the Zel'dovich equation (50) we may readily evaluate the peculiar velocity of the fluid element with Lagrangian coordinate $\mathbf{q}$:

$$\begin{aligned} \mathbf{v} \,=\, a\,\frac{d\,\mathbf{x}}{dt} &= -\,a\dot{D}\;\vec{\nabla}\Psi \\ &= -\,a\,D\,H\;\frac{a\,\dot{D}}{\dot{a}\,D}\;\vec{\nabla}\Psi \end{aligned} \tag{51}$$

yielding the expression

$$\boxed{\mathbf{v} \,=\, -\,aD\,H f(\Omega)\;\vec{\nabla}\Psi} \tag{52}$$

This, in turn, allows us to relate the "displacement potential" Ψ to the gravitational potential perturbation ϕ. We know that in the linear regime the peculiar velocity $\mathbf{v}$ is directly proportional to the peculiar gravity $\mathbf{g}$,

$$\mathbf{v} \,=\, \frac{2f(\Omega)}{3\Omega H}\,\mathbf{g} \,=\, -\frac{2f(\Omega)}{3\Omega H}\;\frac{\nabla\phi}{a} \tag{53}$$

Equating expression (53) to its Zel'dovich equivalent (52) enables us to immediately find the intended relation:

$$\boxed{\Psi(\mathbf{q}) \,=\, \frac{2}{3\,D\,a^2H^2\,\Omega}\;\phi(\mathbf{x},t)} \tag{54}$$

As a consistency dheck we may notice that this implies the potential Ψ to be time-independent. Because according to linear theory the gravitational potential ϕ grows as

$$\begin{aligned} \phi(t) \,=\, \frac{D}{a}\,\phi_0 \quad\Longrightarrow\quad \Psi(\mathbf{q}) &= \frac{2}{3\Omega H^2\,a^3}\;\phi_0 \,=\, \text{const.} \\ &= \frac{2}{3\Omega_0 H_0^2}\;\phi_0 \end{aligned} \tag{55}$$

with ϕ_0 the linearly extrapolated gravitational potential at the current epoch (a=1). This precisely confirms the intended time-independence of Ψ.

4.0.9. Zel'dovich Displacement Vector: Fourier Components

The previous subsection established the relation between displacement potential $\Psi(\mathbf{q})$ and the linearly extrapolated gravitational potential ϕ_0. It is straightforward to use this relation to also find the relation between the displacement vector $\vec{\psi}$,

$$\mathbf{x} \,=\, \mathbf{q} \,-\, D(t)\,\vec{\psi}(\mathbf{q})\,, \tag{56}$$

and the density perturbation field δ, on the basis of the gradient of ϕ_0,

$$\boxed{\vec{\psi}(\mathbf{q}) \,=\, -\,\frac{2}{3\Omega_0 H_0^2}\,\vec{\nabla}\phi_0} \tag{57}$$

This relation allows us to compute the displacement vector $\vec{\psi}$ directly from the density field Fourier components $\hat{\delta}(\mathbf{k})$. Using their Fourier definitions,

$$\vec{\psi}(\mathbf{x}) = \int \frac{d\mathbf{k}}{(2\pi)^3}\ \hat{\vec{\psi}}(\mathbf{k})\ e^{-i\mathbf{k}\cdot\mathbf{x}} \tag{58}$$

$$\phi_0(\mathbf{x}) = \int \frac{d\mathbf{k}}{(2\pi)^3}\ \hat{\phi}_0(\mathbf{k})\ e^{-i\mathbf{k}\cdot\mathbf{x}} \tag{59}$$

which in combination with eqn. (57) leads to the Fourier relation

$$\hat{\vec{\psi}}(\mathbf{k}) = i\,\frac{2}{3\Omega_0 H_0^2}\,\mathbf{k}\,\hat{\phi}_0(\mathbf{k})\,. \tag{60}$$

Earlier, in chapter 5, we had derived the relation between the Fourier components $\hat{\phi}(\mathbf{k})$ and the density fluctuation Fourier components $\hat{\delta}(\mathbf{k})$,

$$\begin{aligned}\hat{\phi}(\mathbf{k}) &= -\frac{3}{2}\,\Omega H^2\,a^2\,\frac{1}{k^2}\,\hat{\delta}(\mathbf{k}) \\ &= -\frac{3}{2}\,\Omega_0 H_0^2\,\frac{1}{a}\,\frac{1}{k^2}\,\hat{\delta}(\mathbf{k})\end{aligned} \tag{61}$$

$$\hat{\phi}_0(\mathbf{k}) = -\frac{3}{2}\,\Omega_0 H_0^2\,\frac{1}{k^2}\,\hat{\delta}_0(\mathbf{k}) \tag{62}$$

in which $\hat{\delta}_0(\mathbf{k})$ and $\hat{\phi}_0(\mathbf{k})$ are the Fourier components of the density perturbation and potential linearly extrapolated to the present epoch. With the help of eqn. (60) we thus find that

$$\boxed{\hat{\vec{\psi}}(\mathbf{k}) = -i\,\frac{\mathbf{k}}{k^2}\,\hat{\delta}(\mathbf{k})} \tag{63}$$

We therefore find the relation between the Zel'dovich displacement field $\vec{\psi}(\mathbf{q})$ and the field of (linearly extrapolated) density perturbations $\delta_0(\mathbf{x})$,

$$\boxed{\vec{\psi}(\mathbf{q}) = \int \frac{d\mathbf{k}}{(2\pi)^3}\,\left\{-i\,\frac{\mathbf{k}}{k^2}\,\hat{\delta}(\mathbf{k})\right\}\,e^{-i\mathbf{k}\cdot\mathbf{q}}} \tag{64}$$

4.0.10. Cosmological N-body Simulations: Initial Conditions

Relation (64) brings us to the highly important application of the Zel'dovich formalism for setting up the initial conditions of N-body simulations of cosmological structure formation.

In the case of N-body simulations the matter distribution is discretized into (nearly pointsized) particles representing cosmic mass elements. Each of them is coded by its initial position, its Lagrangian coordinate $\mathbf{q}$. The conventional strategy is to locate these at the $N = M^3$ gridpoints of a regular cubic

grid. A variety of other techniques such as "glass initial conditions" have attained some popularity to get rid of the salient imprint of the grid, but certainly for the discussion here it is better to keep to the pure grid algorithm. Subsequently these particles are displaced from their primordial grid locations such that the resulting density and velocity perturbation field should adhere to the generated initial random density field $\delta(\mathbf{x}, t)$. It would be unpractical, and almost unfeasible, to accomplish this by directly generating a discrete Poisson sample of this density field.

The strategy based on the Zel'dovich approximation is amazingly efficient. It consists of the following straightforward steps:

- Sample a primordial density field $\delta(\mathbf{x})$ for a (user-specified) cosmological power spectrum $P(k)$. In practice the sampling, on the $N = M^3$ vertices of a specified cubic grid, is easily achieved by generating the mutually independent Gaussian distributed Fourier components of the density field:

$$\hat{\delta}(\mathbf{k}_i) \tag{65}$$

  These Fourier components are generated on the grid locations of the related Fourier grid.

- Compute the displacement field $\vec{\psi}(\mathbf{x})$ at the N gridpoints by using the Fourier integral (64),

$$\vec{\psi}(\mathbf{q}) \,=\, \int \frac{d\mathbf{k}}{(2\pi)^3} \left\{ -i\, \frac{\mathbf{k}}{k^2}\, \hat{\delta}(\mathbf{k}) \right\} \, e^{-i\mathbf{k}\cdot\mathbf{q}} \tag{66}$$

  In practice this involves the use of a Fast Fourier Transform.

- Displace the particles initially at the grid positions $\mathbf{q}$ to their location

$$\mathbf{x}(\mathbf{q}) \,=\, \mathbf{q} \,+\, D(t)\, \vec{\psi}(\mathbf{q})\,, \tag{67}$$

  where we chose the time t such that $D(t) \ll 1$. In practice this Zel'dovich displacement is forwarded to a time t such that the resulting maximum $\delta \approx 1$. These locations $\mathbf{x}(\mathbf{q})$ are the input initial positions for the particles in the N-body simulation.

- Subsequently, each of these particles is also given their initial velocity by means of the corresponding Zel'dovich prescription (52),

$$\mathbf{v}(\mathbf{q}) \,=\, aD\, Hf(\Omega)\, \vec{\psi}(\mathbf{q}) \tag{68}$$

4.0.11. Zel'dovich formalism: Density Evolution

solution for its displacement is based upon the first-order truncation of the Lagrangian perturbation series of the trajectories $\mathbf{x}(\mathbf{q}, t)$ of mass elements from their initial position $\mathbf{q}$, The succesive terms of form a sequence of ordered moments of the displacement $\mathbf{s} = \mathbf{x} - \mathbf{q}$, such that the truncation at the $\mathbf{x}^{(1)}$ term corresponds to the simple linear prescription for the displacement of a particle from its initial (Lagrangian) comoving position $\mathbf{q}$ to an Eulerian comoving position $\mathbf{x}$.

, solely determined by the initial gravitational potential field.

$$\mathbf{x}(\mathbf{q}, t) \,=\, \mathbf{q} \,-\, D(t) \nabla\Psi(\mathbf{q})\,. \tag{69}$$

This

In this mapping, the time dependent function $D(t)$ is the growth rate of linear density perturbations, and the time-independent spatial function $\Psi(\mathbf{q})$ is related to the *linearly extrapolated* gravitational potential $\underline{\phi}$[1],

$$\Psi \,=\, \frac{2}{3Da^2\Omega H^2}\, \underline{\phi}\,. \tag{70}$$

[1] the *linearly extrapolated* gravitational potential is defined as the value the gravitational potential would assume in case the field would evolve according to its linear growth rate, $D(t)/a(t)$

This immediately clarifies that what represents the major virtue of the Zel'dovich approximation, its ability to assess the evolution of a density field from the primordial density field itself, through the corresponding linearly extrapolated (primordial) gravitational potential. While in essence a local approximation, the Lagrangian description provides the starting point for a far-reaching analysis of the implied density field development,

$$\frac{\rho(\mathbf{x},t)}{\rho_u} \;=\; \left\| \frac{\partial \mathbf{x}}{\partial \mathbf{q}} \right\|^{-1} \;=\; \left\| \delta_{mn} - a(t)\psi_{mn} \right\|^{-1} \;=\; \frac{1}{[1-a(t)\lambda_1][1-a(t)\lambda_2][1-a(t)\lambda_3]}\,, \tag{71}$$

where the vertical bars denote the Jacobian determinant, and λ_1, λ_2 and λ_3 are the eigenvalues of the Zel'dovich deformation tensor ψ_{mn},

$$\psi_{mn} \;=\; \frac{D(t)}{a(t)}\,\frac{\partial^2 \Psi}{\partial q_m \partial q_n} \;=\; \frac{2}{3a^3\Omega H^2}\,\frac{\partial^2 \underline{\phi}}{\partial q_m \partial q_n}\,, \tag{72}$$

which also implies the deformation matrix ψ_{mn} and its eigenvalues to evolve as $\psi_{mn} \propto D(t)/a(t)$. On the basis of above relation, it is then straightforward to find the intrinsic relation between the Zel'dovich deformation tensor ψ_{mn} and the tidal tensor T_{mn},

$$\psi_{mn} \;=\; \frac{1}{\frac{3}{2}\Omega H^2 a}\Big(\, \underline{T}_{mn} \;+\; \tfrac{1}{2}\Omega H^2\, \underline{\delta}\, \delta_{mn} \,\Big)\,, \tag{73}$$

where $\underline{\delta}$ and $\underline{T}_{mn}$ are the respective *linearly extrapolated* values of these quantities, i.e. $\underline{\delta}(t) \propto D(t)$ and $\underline{T}_{mn} \propto D/a^3$. Notice that, without loss of generality, we can adopt a coordinate system where the tidal tensor matrix T_{mn} is diagonal, from which we straightforwardly find a relation between the linearly extrapolated $\underline{\delta}$ and the deformation tensor, $\underline{\delta}(t) = a(t)\sum_m \lambda_m$.

For appreciating the nature of the involved approximation, one should note that the continuity equation (by definition) is always satisfied by the combination of the Zel'dovich approximation and the mass conservation, yet that they do not, in general, satisfy the Euler and the Poisson equations (Nusser et al. 1991). Only in the case of purely one-dimensional perturbations does the Zel'dovich approximation represent a full solution to all three dynamic equations. Indeed, as we will emphasize in section 3.5.2, the core and essential physical significance of the Zel'dovich approximation can be traced to this implicit assumption of the tidal tensor T_{ij} being linearly proportional to the deformation tensor, and hence the velocity shear tensor.

The central role of the Zel'dovich formalism (for a review, see Shandarin & Zel'dovich 1989) in structure formation studies stems from its ability to take any arbitrary initial random density field, not constrained by any specific restriction in terms of morphological symmetry or seclusion, and mould it through a simple and direct operation into a reasonable approximation for the matter distribution at later nonlinear epochs. It allows one to get a rough qualitative outline of the nonlinear matter distribution solely on the basis of the given initial density field. While formally the Zel'dovich formalism comprises a mere first order perturbative term, it turned out to represent a surprisingly accurate description up to considerably more advanced evolutionary stages, up to the point where matter flows would start to cross each other.

4.1. General Lagrangian Formalism

Hui & Bertschinger (1996) demonstrated how the Zel'dovich approximation can be incorporated within this context of reducing the problem to a local one by invoking a specific approximation. In essence it involves an implicit decision to discard H_{ij} and the full evolution equation for T_{ij} altogether and replace

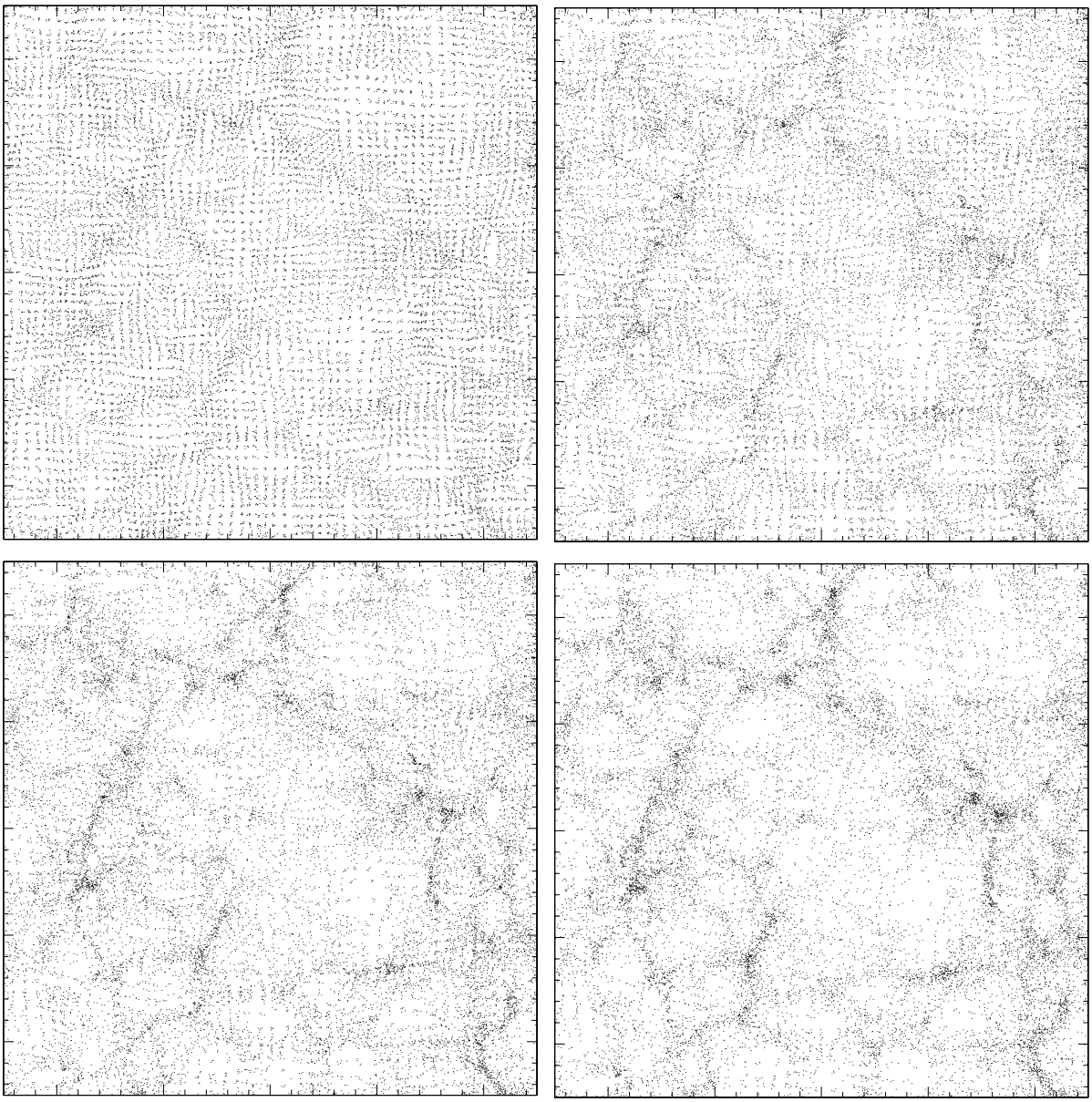

Figure 2. Zel'dovich displaced particle distributions inferred from an unconstrained random realization of a primordial matter distribution for a SCDM cosmological scenario in a $50h^{-1}$Mpc. Time sequence from top left to bottom right, frames corresponding to cosmic epochs $a = 0.10, 0.15, 0.20$ and 0.25.

it by the explicit expression for the evolution of the tidal tensor T_{ij} in the linear regime of clustering, in which T_{ij} is linearly proportional to the shear σ_{ij},

$$T_{ij} \;=\; -\frac{3\Omega H^2}{2Hf(\Omega)}\;\sigma_{ij} \tag{74}$$

where $f(\Omega) \approx \Omega^{0.6}$. From this consideration we can straightforwardly appreciate that the Zel'dovich approximation does not obey the Poisson equation. As a consequence, it does represent an exact approximation in the case of a plane-parallel density disturbance as long as the corresponding particle trajectories have not yet intersected others, but breaks down in the case of two- or three-dimensional perturbations and in general as soon as the particle tracks have crossed. One well-known implication is that the Zel'dovich approximation gives incorrect results for spherical infall.

4.2. Higher-Order Lagrangian Approximations

With the Zel'dovich approximation basically concerning the first order solution in Lagrangian perturbation theory, various extensions and elaborations were formulated attempting to extend the theory to a higher order, futhering its range of applicability towards more evolutionary more progressive situations. As can be appreciated from Eqn. (#), the Zel'dovich approximation essentially involves a truncation of the set of Lagrangian fluid equations through an implicit choice for T_{ij}, equating it linearly proportional to σ_{ij}. This implies a tinkering with the Raychaudhury and shear evolution equations. In the Zel'dovich approximation one therefore need not integrate the tidal evolution equation, the gravity field on a mass element given by a simple extrapolation of initial conditions.

Pursuing along the same track, Bertschinger & Jain (1994) and Hui & Bertschinger (1996) extended this to higher-order schemes, both approximations involving the integration of the exact Raychaudhuri and shear evolution and shifting the approximation to the level of the tidal evolution equation. Bertschinger & Jain (1994) tried to make the very specific assumption of setting the magnetic part of the Weyl tensor $H_{ij} = 0$, thus characterized as the "nonmagnetic" approximation. Subsequent work showed that this does not adhere to a well-defined or easily recognizable generic situation. Along the same lines, Hui & Bertschinger (1996) defined another approximate scheme, the "local tidal" approximation. This they showed to followed more accurately the predictions of the homogeneous ellipsoidal model than the "nonmagnetic" approximation (Bertschinger & Jain 1996) and the Zel'dovich approximation. Interestingly, while the "nonmagnetic" approximation implied collapse into "spindle" like configurations as the generic outcome of gravitational collapse, the more accurate "local tidal" approximation appears to agree with the Zel'dovich approximation in that "planar" geometries are more characteristic.

A range of additional approximate schemes, mostly stemming from different considerations, were introduced in a variety of publications. Most of them try to deal with the evolution of high-density regions after the particle trajectories cross and self-gravity of the resulting matter assemblies assumes a dominating role. Notable examples of such approaches are the adhesion approximation (Kofman, Pogosyan & Shandarin 1990), the frozen flow approximation (Matarrese et al. 1992), the frozen potential approximation (Brainerd, Scherrer & Villumsen 1993), the truncated Zel'dovich approximation (Coles, Melott & Shandarin 1993), the smoothed potential approximation (Melott, Sathyaprakash & Sahni 1996) and higher order Lagrangian perturbation theory (Melott, Buchert & Weiss 1995). The elegant generalization of the Zel'dovich approximation by Giavalisco et al. (1993) will be described later within the context of the mixed boundary conditions problem (next section). An extensive and balanced review of the various approximation schemes may be found in Sahni & Coles (1995).

4.3. Mixed Boundary Conditions

For pure theoretical purposes, cosmological studies may be restricted to considerations involving pure *initial conditions* problems. For a given cosmological and structure formation model the initial density and velocity field are specified, and its evolution subsequently evolved, either by means of approximate

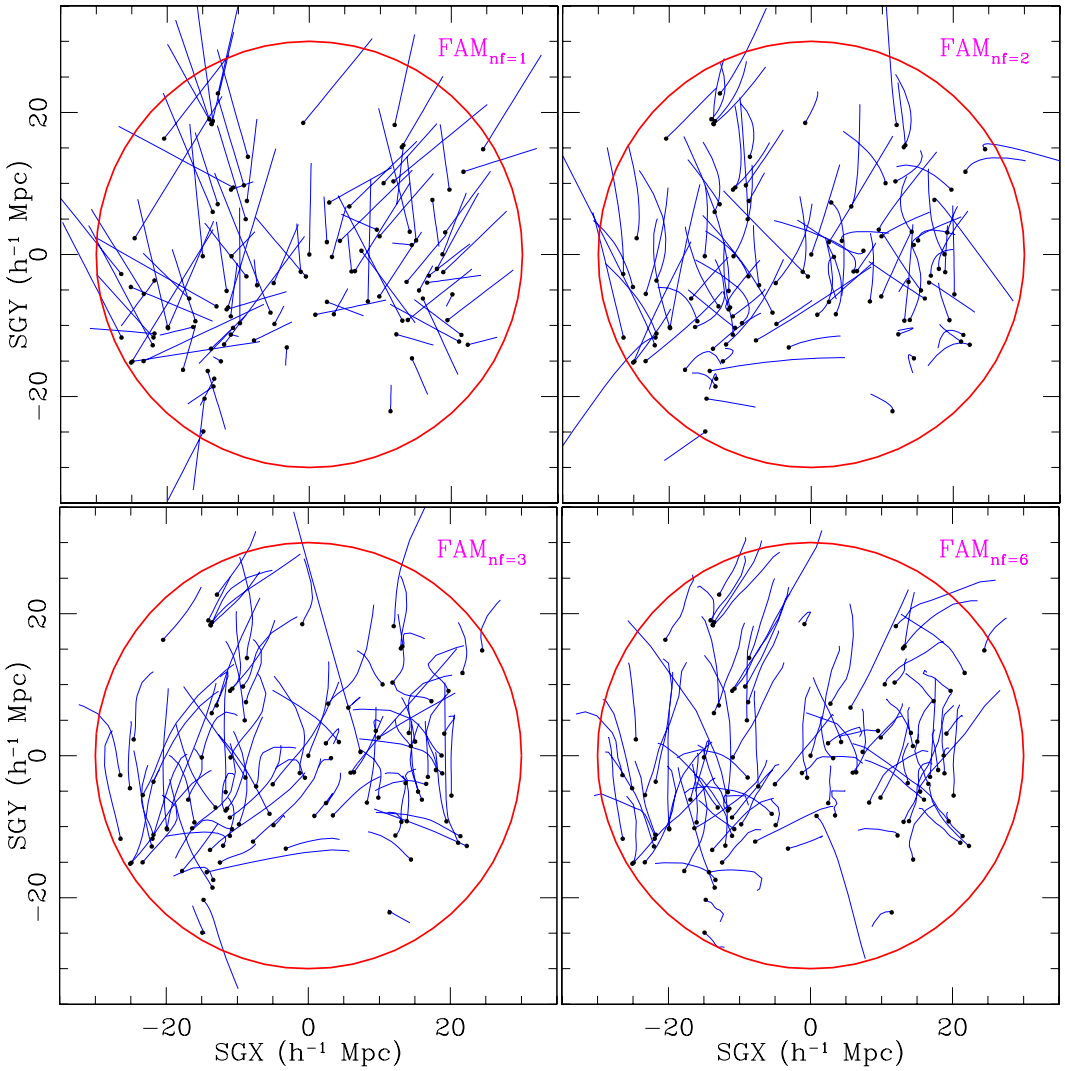

Figure 3. Projected orbits reconstructed by the Fast Action Method implementation of the Least Action Principle procdure. Four different levels of approximation are shown. The black dots represent the final (present) positions for each object. The blue lines indicate the trajectories followed by the objects as a function of time. The top-left frame shows FAM reconstructed orbits with $N_f = 1$ (Zel'dovich approximation). Subsequently shown are $N_f = 2$ (top right), $N_f = 3$ (lower left) and $N_f = 6$ (lower right). From Romano-Díaz, Branchini & van de Weygaert 2002.

schemes or by for instance by means of fully nonlinear N-body computer simulations. The outcome of such studies are then usually analyzed in terms of a variety of statistical measures. These are then compared to the outcome of the same tests in the case of the observed world.

Alternatively, we may recognize that in many specific cosmological studies we are dealing with problems of *mixed boundary conditions*. Part of the large scale structures and velocities in the universe may have been measured at the present epoch, while some in the limit of very high redshift (e.g. the CMB). Typically, one seeks to compute the velocity field consistent with an observed density structure at the present epoch. Conversely, one may wish to deduce the density from the measured peculiar galaxy velocities. Evidently, the position and velocities of objects at the present epoch are intimately coupled through the initial conditions.

In the linear regime, the problem of mixed boundary conditions is easily solved. However, in the case of the interesting features in e.g. the cosmic foam the density of galaxies can reach values considerably larger than unity, even on scales of $\sim 10h^{-1}$Mpc. The associated velocities therefore need to be computed nonlinearly. As may be obvious from the earlier discussions, the nonlinear computation of gravitational instabilities in the case of arbitrary configurations is everything but trivial.

N-body codes are rendered obsolete in such issues involving mixed boundary conditions. Their application is restricted to initial value problems. A further complication of the nonlinear problem of mixed boundary conditions is the multivalued nature of the solutions. Orbit crossing makes identification of the correct orbits difficult, and impossible after virialization has erased the memory of the initial conditions. In practice, one is therefore often restricted to laminar flow in the quasi-linear regime. Perturbations may have exceeded unity but orbit crossing has not yet obstructed a one-to-one correspondence between the final and initial positions. Evidently, the Zel'dovich approximation forms a good first-order approach towards dealing with such issues. Following this, it was applied to the nonlinear problem of mixed boundary conditions, tested and calibrated using N-body simulations, by Nusser et al. (1991) and Nusser & Dekel (1992).

In terms of the physics of the nonlinear systems, a profound suggestion was forwarded by Peebles (1989, 1990). He noticed that mixed boundary conditions naturally lend themselves to an application of Hamilton's principle. Given the action S of a system of particles

$$S \;=\; \int_0^{t_0} L dt \;=\; \int_0^{t_0} dt \;\sum_i \,[\,\frac{1}{2} m_i a^2 \dot{\mathbf{x}}_i^2 - m_i \phi(\mathbf{x}_i)\,]\;, \tag{75}$$

in which L is the Lagrangian for the orbits of particles with masses m_i and comoving coordinates x_i. The *exact* equations of motion for the particles can be obtained from stationary variations of the action S. On the basis of Hamilton's principel one therefore seeks stationary variations of an action subject to fixed boundary conditions at both the initial and final time. Confining oneself to feasible approximate evaluation in this *Least Action Principle* approach, one describes the orbits of particles as a linear combination of suitably chosen universal functions of time with unknown coefficients specific to each particle presently located at a position $\mathbf{x}_{i,0}$,

$$\mathbf{x}_i(D) \;=\; \mathbf{x}_{i,0} \;+\; \sum_{n=1}^{N_f} \,q_n(D)\;\mathbf{C}_{i,n}\;. \tag{76}$$

In the above formulation we choose to use the linear growth mode $D(t)$ as time variable. The functions $q_n(D)$ form a set of N_f time-dependent basis functions, while $\mathbf{C}_{i,n}$ are a set of free parameters which are determined from evaluating the stationary variations of the action. The basis functions $q_n(D)$ are constrained by two orbital constraints. To ensure that at the present time the galaxies are located at their observed positions $\mathbf{x}_i(D=1) = \mathbf{x}_{i,0}$ we set the boundary constraint $q_n(1) = 0$. The other boundary condition concerns the constraint that the peculiar motions at early epochs ($D = 0$) have to vanish, which in turn ensures initial homogeneity, i.e. $\lim_{t\rightarrow 0} m_i a^2 \dot{\mathbf{x}}_i = 0$. The choice of base functions essentially determines the approximation scheme. Originally Peebles (1989, 1990) chose the base functions $q_n(D) = f_n(t)$ to be polynomials of the expansion factor $a(t)$. For small systems this leads to a tractable problem,

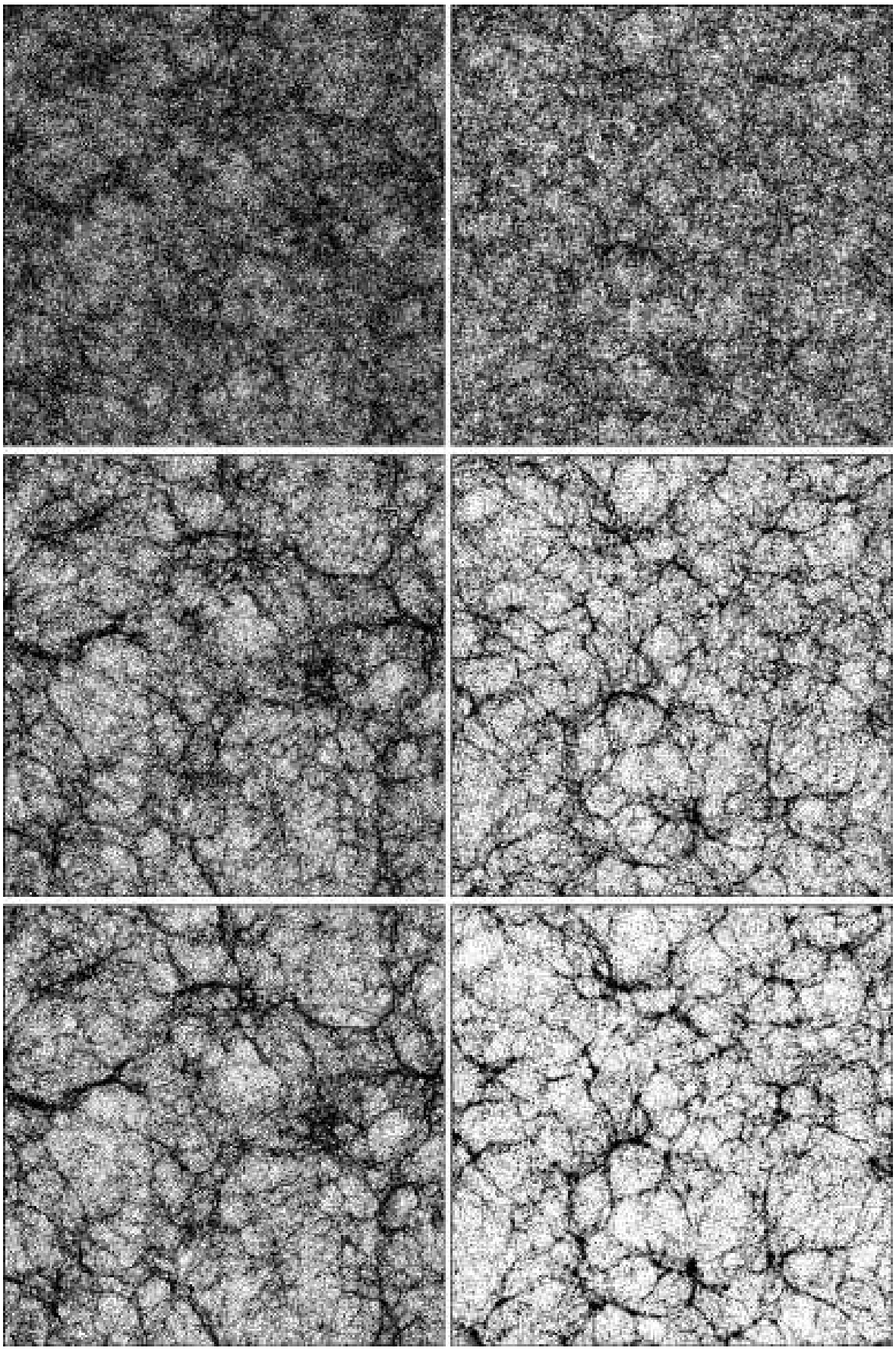

Figure 4. Gravitational clustering in scale-free scenarios. Left: $n = -2$ simulation, at $a = 0.2, 0.45, 0.55$. Right: $n = 1.5$ at $a = 0.25, 0.63, 1.0$. From Smith et al. 2003.

but for larger systems it becomes exceedingly difficult to apply because of confusions between multivalued solutions. In an elegant contribution, Giavalisco et al. (1993) merged the Zel'dovich approximation into the *Least Action Principle* (LAP) scheme by expanding the formalism into one where the base functions are higher order polynomials of the linear growth function $D(t)$. In the limit of small displacements, the LAP procedure would then reproduce the Zel'dovich approximation. The higher order terms remove the separability of the temporal and spatial dependence in the Zel'dovich approximation, and allowing arbitrary displacements so that the orbits can be determined to any accuracy. This turned out to yield a rapidly converging scheme, even for highly nonlinear perturbations.

A further improvement of the basic scheme of Giavalisco et al. (1993) was introduced by Nusser & Branchini (2000). They based their computational evaluations of the action on invoking the functions $p_n(D) \equiv dq_n/dD$ and setting them equal to conveniently defined polynomials of the growth factor D. In addition, their *Fast Action Method* (FAM) involved a computational optimization through the evaluation of the gravitational potential by means of a gravitational TREECODE. This yielded a procedure allowing the reconstruction of the orbits of $10^4 - 10^5$ mass tracing objects back in time and reconstruct the peculiar velocities of the objects well beyond the linear regime. Its performance can be appreciated from Figure # (from Romano-Díaz, Branchini & van de Weygaert 2004), in which 4 panels show how the increasing levels of orbit expansion manage to probe ever deeper into the nonlinear regime. In particular, one can infer how the Zel'dovich approximation is naturally invoked as the 1st-order step (top left panel).

5. Spherical Model

Analytically tractable idealizations help to understand various aspects of void evolution. In this regard, the *spherical model* represents the key reference model against which we may assess the evolution of more complex configurations. Also, it provides the clearest explanation for the various void characteristics listed in the main test. And most significantly within the context of this work, it provides the fundament from which our formalism for hierarchical void evolution is developed.

The structure of a spherical void or peak can be treated in terms of mass shells. In the "spherical model" concentric shells remain concentric and are assumed to be perfectly uniform, without any substructure. The shells are supposed never to cross until the final singularity, a condition whose validity is determined by the initial density profile. The resulting solution of the equation of motion for each shell may cover the full nonlinear evolution of the perturbation, as long as shell crossing does not occur.

The treatment of the spherical model in a cosmological context has been fully worked out (Gunn & Gott 1973; Lilje & Lahav 1991). As long as the mass shells do not cross, they behave as mini-Friedmann universes whose equation of motion assumes exactly the same form as that of an equivalent FRW universe with a modified value of Ω_s. The details of the distribution of the mass interior to the shell are of no direct relevance to the evolution of each individual shell. Instead, the evolution depends on the total mass contained within the radius of the shell. and the global cosmological background density.

Although quantitative details depend on the cosmological model, a study of the evolution of spherical perturbations in an Einstein-de Sitter Universe suffices to illustrate all the important physical features.

5.1. Definitions

When a mass shell at some initial time t_i starts expanding from a physical radius $r_i = a(t_i)x_i$, its subsequent motion is characterized by the expansion factor $\mathcal{R}(t, r_i)$ of the shell:

$$r(t, r_i) = \mathcal{R}(t, r_i) r_i \,, \tag{77}$$

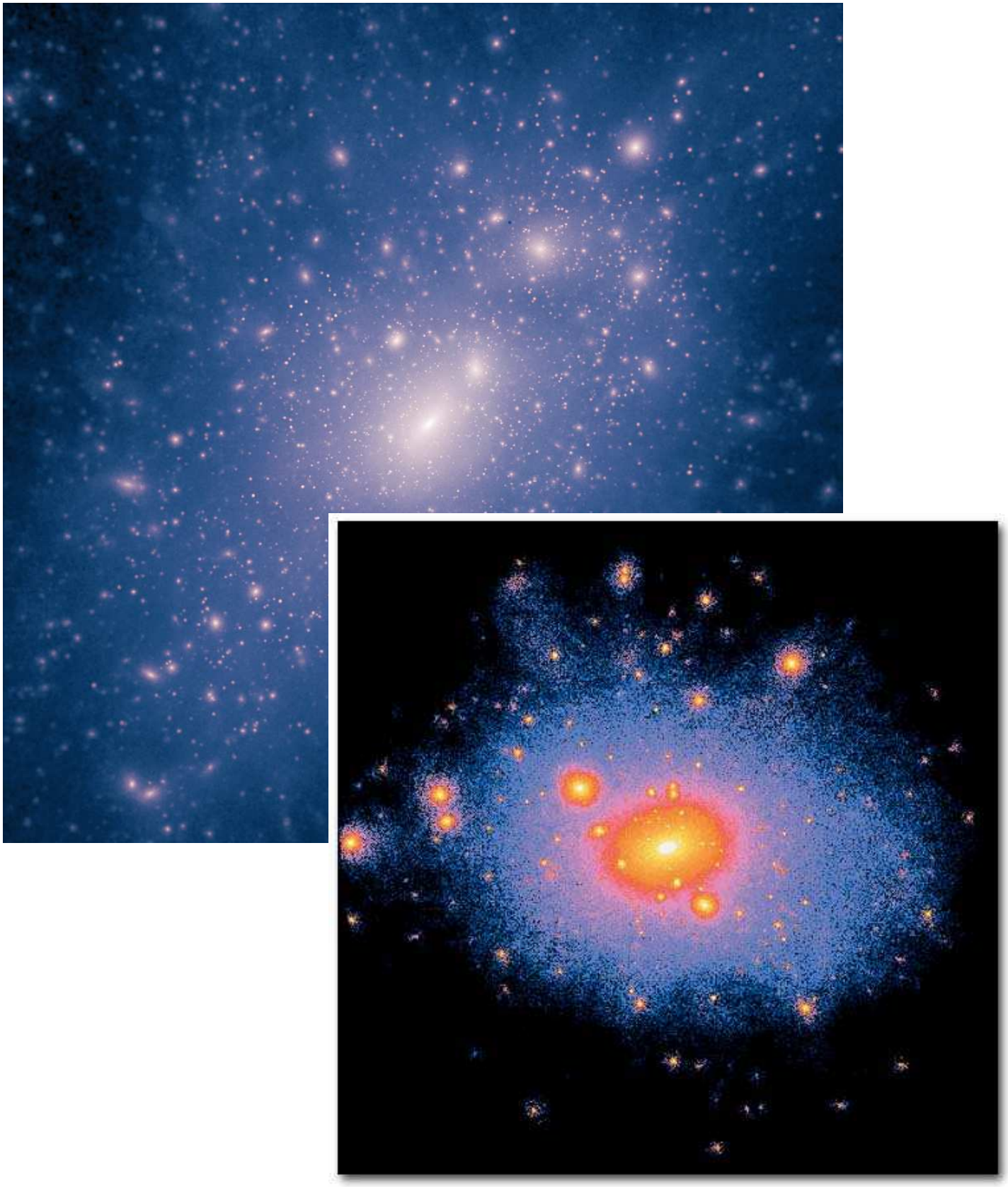

Figure 5. Similarity in the cosmic structure formation process: the formation of a cluster (from very high resolution simulation by V. Springel) and of a galaxy (T. Quinn), both in ΛCDM scenario.

where $r(t, r_i) = a(t)x(t, x_i)$ is the physical radius of the shell at time t and $x(t, x_i)$ the corresponding comoving radius. The evolution of the shell is dictated by the cosmological density parameter

$$\Omega(t) \, = \, \frac{8\pi G \, \rho_u(t)}{3H_u^2} \tag{78}$$

and the mean density contrast within the radius of the shell,

$$\begin{aligned} \Delta(r,t) &= \frac{3}{r^3}\int_0^r \left[\frac{\rho(y,t)}{\rho_u(t)} - 1\right] \, y^2 \, dy \\ &= \frac{3}{r^3}\int_0^r \delta(y,t)\, y^2 \, dy \, , \end{aligned} \tag{79}$$

To determine the evolution of $R(t, r_i)$, it is convenient to introduce the parameters $\Delta_{ci} = \Delta_c(t_i)$ and α_i where

$$\begin{aligned} 1 + \Delta_{ci} &= \Omega_i \, [1 + \Delta(t_i, r_i)] \\ \alpha_i &= \left(\frac{v_i}{H_i r_i}\right)^2 - 1 \, . \end{aligned} \tag{80}$$

Here, $\Omega_i = \Omega(t_i)$, $H_i = H(t_i)$ and v_i is the physical velocity (i.e. the sum of the peculiar velocity and Hubble expansion velocity with respect to the void center) of the mass shell at $t = t_i$. The usual assumption of a growing mode perturbation implies that the velocity perturbation $v_{pec,i}$ for a spherical perturbation, at the initial time t_i, is

$$v_{pec,i} \, = \, -\frac{H_i r_i}{3} f(\Omega_i) \Delta(r_i, t_i) \, , \tag{81}$$

and hence,

$$\alpha_i \, = \, -\frac{2}{3} f(\Omega_i) \Delta(r_i, t_i) \, . \tag{82}$$

In effect, Δ_{ci} is the density contrast of the shell with respect to a critical universe ($\Omega = 1$) at the cosmic time t_i, while α_i is a measure of the corresponding peculiar velocity (or, rather, the kinetic energy) of the shell. The evolution of a spherical over- or underdensity is *entirely* and *solely* determined by the initial (effective) over- or underdensity within the (initial) radius r_i of the shell, $\Delta_{ci}(r_i, t_i)$, and the corresponding velocity perturbation, $v_{pec,i}$. Hence, the values of Δ_{ci} and α_i determine whether a shell will stop expanding or not, i.e. whether it is closed, critical or open. The criterion for a closed shell is $\Delta_{ci} > \alpha_i$, for a critical shell, $\Delta_{ci} = \alpha_i$, and $\Delta_{ci} < \alpha_i$ for an open shell.

Notice that these expressions assume that the initial density fluctuation was negligible, so that the initial mass m and initial comoving size R are related: $m \propto R^3$.

5.2. Shell Solutions

The solution for the expansion factor $\mathcal{R}(t, r_i) = \mathcal{R}(\Theta_r)$ of an overdense cq. underdense shell is given by the parametized expressions

$$\mathcal{R}(\Theta_r) \, = \, \begin{cases} \frac{1}{2}\, \dfrac{1 + \Delta_{ci}}{(\alpha_i - \Delta_{ci})} \; (\cosh\Theta_r - 1) & \Delta_{ci} < \alpha_i, \\ \\ \frac{1}{2}\, \dfrac{1 + \Delta_{ci}}{(\Delta_{ci} - \alpha_i)} \; (1 - \cos\Theta_r) & \Delta_{ci} > \alpha_i \, , \end{cases} \tag{83}$$

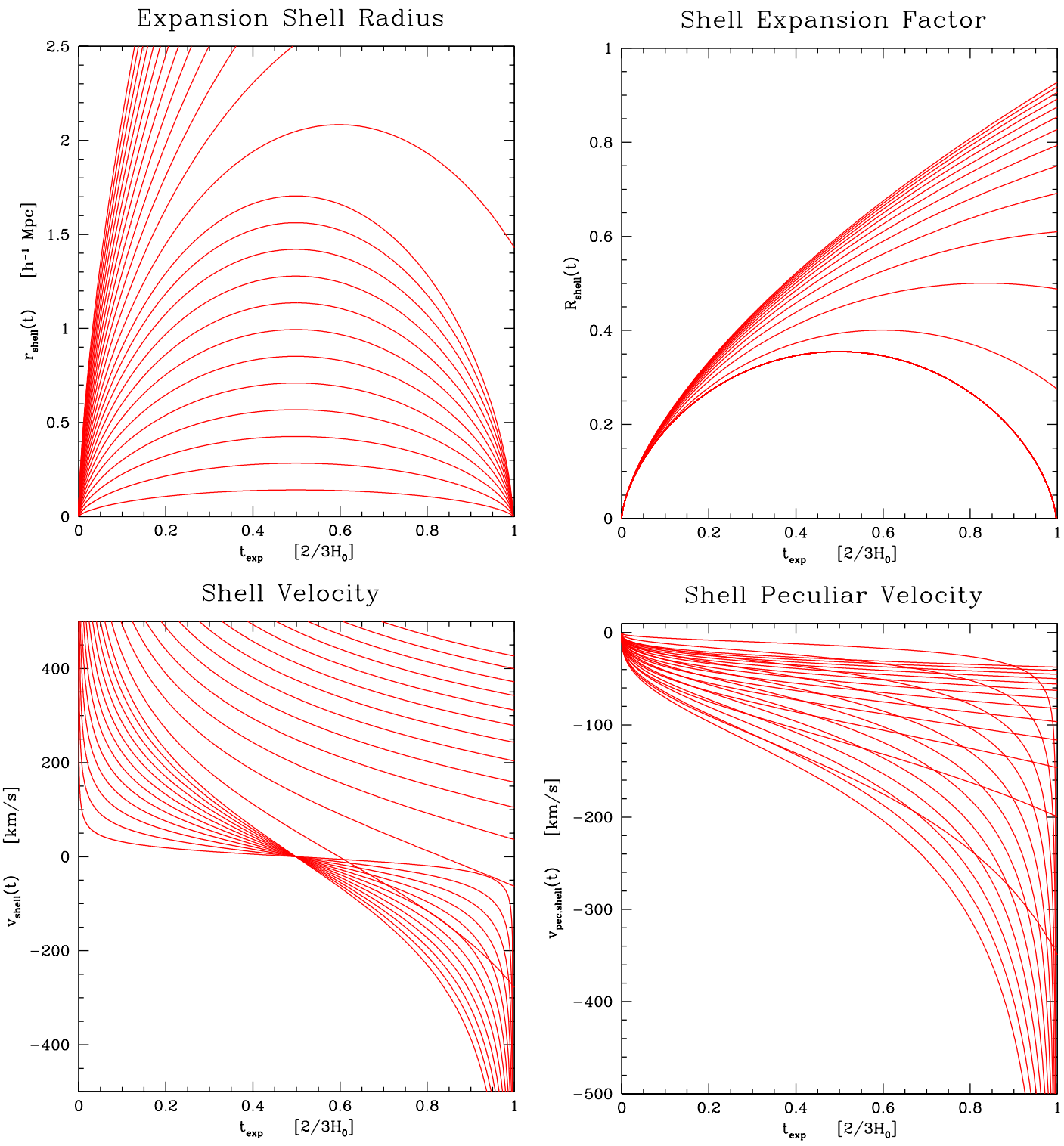

Figure 6. Spherical Peak 1

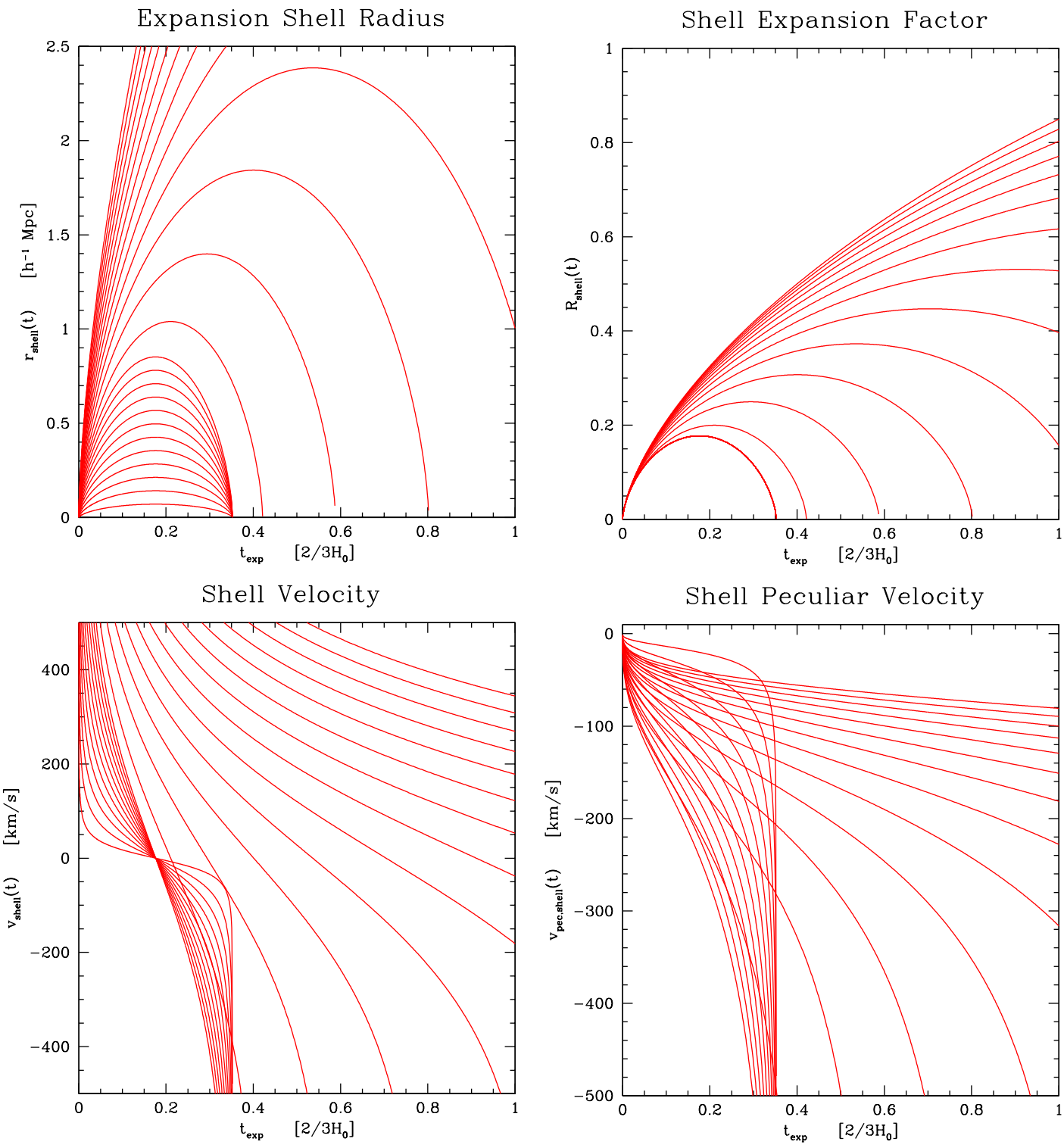

Figure 7. Spherical Peak 2

in which the development angle Θ_r, which paramaterizes all physical quantities relating to the mass shell, is related to time t via

$$t(\Theta_r) \;=\; \begin{cases} \frac{1}{2}\,\dfrac{1+\Delta_{ci}}{(\alpha_i-\Delta_{ci})^{3/2}}\;\;(\sinh\Theta_r-\Theta_r) & \Delta_{ci}<\alpha_i \\ \\ \frac{1}{2}\,\dfrac{1+\Delta_{ci}}{(\Delta_{ci}-\alpha_i)^{3/2}}\;\;(\Theta_r-\sin\Theta_r) & \Delta_{ci}>\alpha_i \end{cases} \tag{84}$$

while for a critical shell the solution is given by the direct relation

$$\mathcal{R}(\Theta_r) \;=\; \left\{\frac{3}{2}H_i(1+\Delta_{ci})^{1/2}t\right\}^{2/3} \qquad\qquad \Delta_{ci}=\alpha_i\,. \tag{85}$$

Notice that the solutions for the evolution of overdense and underdense regions in essence are the same, and are interchangeable by replacing

$$\begin{aligned} (\sinh\Theta-\Theta) \quad &\Rightarrow \quad (\Theta-\sin\Theta) \\ (\cosh\Theta-1) \quad &\Rightarrow \quad (1-\cos\Theta)\,. \end{aligned} \tag{86}$$

5.3. Density Evolution

If the initial density contrast of a shell is $\Delta_i(r_i)$, its density contrast $\Delta(r,t)$ at any subsequent time t is given by

$$1+\Delta(r,t) \;=\; \frac{1+\Delta_i(r_i)}{\mathcal{R}^3}\,\frac{a(t)^3}{a_i^3}\,, \tag{87}$$

With $\Delta(r,t)$ being a relative quantity, comparing the density of the mass shell at radius r at time t with that of the global cosmic background, the value of $\Delta(r,t)$ is a function of the shell's development angle Θ_r as well as that of the development angle of the Universe Θ_u,

$$\Omega \;=\; \begin{cases} \dfrac{2}{\cosh\Theta_u+1} & \Omega<1, \\ \\ \dfrac{2}{\cos\Theta_u+1} & \Omega>1. \end{cases} \tag{88}$$

The shell's density contrast may then be obtained from

$$1+\Delta(r,t)=f(\Theta_r)/f(\Theta_u), \tag{89}$$

where $f(\Theta)$ is the cosmic "density" function:

$$f(\Theta) \;=\; \begin{cases} \dfrac{(\sinh\Theta-\Theta)^2}{(\cosh\Theta-1)^3} & \text{open}\,, \\ \\ 2/9 & \text{critical}\,, \\ \\ \dfrac{(\Theta-\sin\Theta)^2}{(1-\cos\Theta)^3} & \text{closed}\,, \end{cases} \tag{90}$$

This expression is equally valid for the shell (in which case "open" means $\Delta_{ci}<\alpha_i$) and the global background Universe (where "open" means $\Omega<1$).

5.4. Shell Velocities

The velocity of expansion or contraction of a spherical shell is given by computing $\mathrm{d}\mathcal{R}/\mathrm{d}t$, so it can be written in terms of Θ_r and Θ_u. In particular, the shell's peculiar velocity with respect to the global Hubble velocity,

$$v_{pec}(r,t) \;=\; v(r,t) - H_u(t) r(t)\,, \tag{91}$$

may be inferred from the expression

$$v_{pec}(r,t) \;=\; H_u(t) r(t) \left\{ \frac{g(\Theta_r)}{g(\Theta_u)} \;-\; 1 \right\}\,, \tag{92}$$

where $H_u(t) r = (\dot{a}/a) r$ and the cosmic "velocity" function is

$$g(\Theta) \;=\; \begin{cases} \dfrac{\sinh\Theta\,(\sinh\Theta - \Theta)}{(\cosh\Theta - 1)^2} & \text{open}\,, \\[2ex] \dfrac{2}{3} & \text{critical}\,, \\[2ex] \dfrac{\sin\Theta\,(\Theta - \sin\Theta)}{(1-\cos\Theta)^2} & \text{closed} \end{cases} \tag{93}$$

Thus, we may define a Hubble parameter H_s for each individual shell,

$$H_s(r,t) \;\equiv\; \frac{\dot{\mathcal{R}}}{\mathcal{R}} \;=\; H_u(t) \left\{ \frac{g(\Theta_r)}{g(\Theta_u)} \right\}\,. \tag{94}$$

5.5. Overdensities and collapse when $\Omega = 1$

The previous sections provided explicit expressions for the evolution of a spherical perturbation in FRW backgrounds with no cosmological constant. To better illustrate our argument, we will now specialize to the case of an Einstein de-Sitter model. It will prove useful to contrast the spherical evolution with that predicted by linear theory. We will use $D(z)$ to denote the *linear density perturbation growth factor*, normalized so that $D(z=0) = 1$. For an Einstein-de Sitter Universe,$D(z) = 1/(1+z)$. Note that this makes $D \propto (t/t_0)^{2/3}$. Similarly, the growth of velocities in linear theory is given by

$$v_{\rm lin}(r) \;=\; -\frac{H_u r}{3}\, f(\Omega)\, \Delta(r,t)\,, \tag{95}$$

where $f(\Omega) \approx \Omega^{0.6}$ (Peebles 1980). It is a useful exercise to verify that, in its early stages (i.e., small development angle), the spherical evolution model does indeed reproduce linear theory.

Consider the evolution of an initially overdense (or, rather, bound) shell. Such a shell will initially expand slightly slower than the background, this expansion gradually slowing to a complete halt, after which it turns around and starts to contract. At turnaround, $v(r,t) = 0$, so $\Theta_r = \pi$, and the density is

$$1 + \Delta(r, t_{ta}) = (3\pi/4)^2. \tag{96}$$

Therefore, at turnaround, the *comoving radius* of a spherical perturbation has shrunk by a factor of $(3\pi/4)^{2/3} = 1.771$ from what it was initially. Had the perturbation evolved according to linear theory, then turnaround would happen at that redshift when the linear theory prediction Δ_{lin}, reaches the value $\delta_{\rm ta}$:

$$\Delta_{lin}(z_{\rm ta}) = \delta_{\rm ta} = (3/5)(3\pi/4)^{2/3} \approx 1.062. \tag{97}$$

Full collapse is associated with $\Theta_r = 2\pi$. At this time, the linearly extrapolated initial overdensity reaches the threshold value $\delta_{\rm c}$,

$$\Delta_{lin}(z_{\rm c}) = \delta_{\rm c} = \left(\frac{3}{5}\right)\left(\frac{3\pi}{2}\right)^{2/3} \;\approx\; 1.686\,. \tag{98}$$

This makes it straightforward to determine the collapse redshift $z_{\rm coll}$ of each bound perturbation directly from a given initial density field. In terms of the primordial field linearly extrapolated to the present time, $\Delta_{lin,0}$, the collapse redshift $z_{\rm coll}$ may be directly inferred from

$$D(z_{\rm coll})\,\Delta_{lin,0} \;=\; \delta_{\rm c}\;. \tag{99}$$

so

$$1 + z_{coll} \;=\; \frac{\Delta_{lin,0}}{1.686}. \tag{100}$$

Formally, at collapse, the comoving radius is vanishingly small ($\mathcal{R}(2\pi) = 0$). In reality, the matter in the collapsing object will virialize as interactions between matter in the shells will exchange energy betwen the shells and ultimately an equilibrium distribution will be found. Therefore, it is usual to assume that the final size of a collapsed spherical object is finite and equal to its virial radius. For a perfect *tophat* density, the object's final size $R_{\rm fin}$ is then ≈ 5.622 times smaller than it was initially (Gunn & Gott 1973), i.e.

$$R_{\rm fin}/\widetilde{R}_{i,coll} \;=\; (18\pi^2)^{1/3} \;\approx 5.622\,, \tag{101}$$

where $\widetilde{R}_{i,coll} \equiv R_i(a_{coll}/a_i)$.

5.6. Underdensities and shell-crossing when $\Omega = 1$

Underdense spherical regions evolve differently than their overdense peers. The outward directed peculiar acceleration is directly proportional to the integrated density deficit $\Delta(r,t)$ of the void. In the generic case, the inner shells "feel" a stronger deficit, and thus a stronger outward acceleration, than the outer shells.

Once again, to better illustrate our argument, we will now specialize to the case of an Einstein de-Sitter model. The density deficit evolves as

$$1 + \Delta(r,z) \approx \frac{9}{2}\,\frac{(\sinh\Theta_r - \Theta_r)^2}{(\cosh\Theta_r - 1)^3}. \tag{102}$$

In comparison, the corresponding linear initial density deficit $\Delta_{lin}(z)$:

$$\Delta_{lin}(z) = \frac{\Delta_{lin,0}}{1+z} \approx -\frac{3}{4}^{2/3}\,\frac{(\sinh\Theta_r - \Theta_r)^{2/3}}{5/3}\,. \tag{103}$$

The (peculiar) velocity with which the void expands into its surroundings is

$$v_{pec}(r,t) \;=\; H_u r\,\left\{\frac{3}{2}\frac{\sinh\Theta_r\,(\sinh\Theta_r - \Theta_r)}{(\cosh\Theta_r - 1)^2} \;-\; 1\right\}\,. \tag{104}$$

As a consequence of the differential outward expansion within and around the void, and the accompanying decrease of the expansion rate with radius r, shells start to accumulate near the boundary of the void. The density deficit $|\Delta(r)|$ of the void decreases as a function of radius r, down to a minimum at the center. Shells which were initially close to the centre will ultimately catch up with the shells further outside, until they eventually pass them. This marks the event of *shell crossing*. The corresponding gradual increase of density will then have turned into an infinitely dense ridge. From this moment onward the evolution of the void may be described in terms of a self-similar outward moving shell (Suto et al. 1984; Fillmore & Goldreich 1984; Bertschinger 1985). Strictly speaking, this only occurs for voids whose density profile is sufficiently steep, since a sufficiently strong differential shell acceleration must be generated. This condition is satisfied at the step-function density profile near the edge of a tophat void.

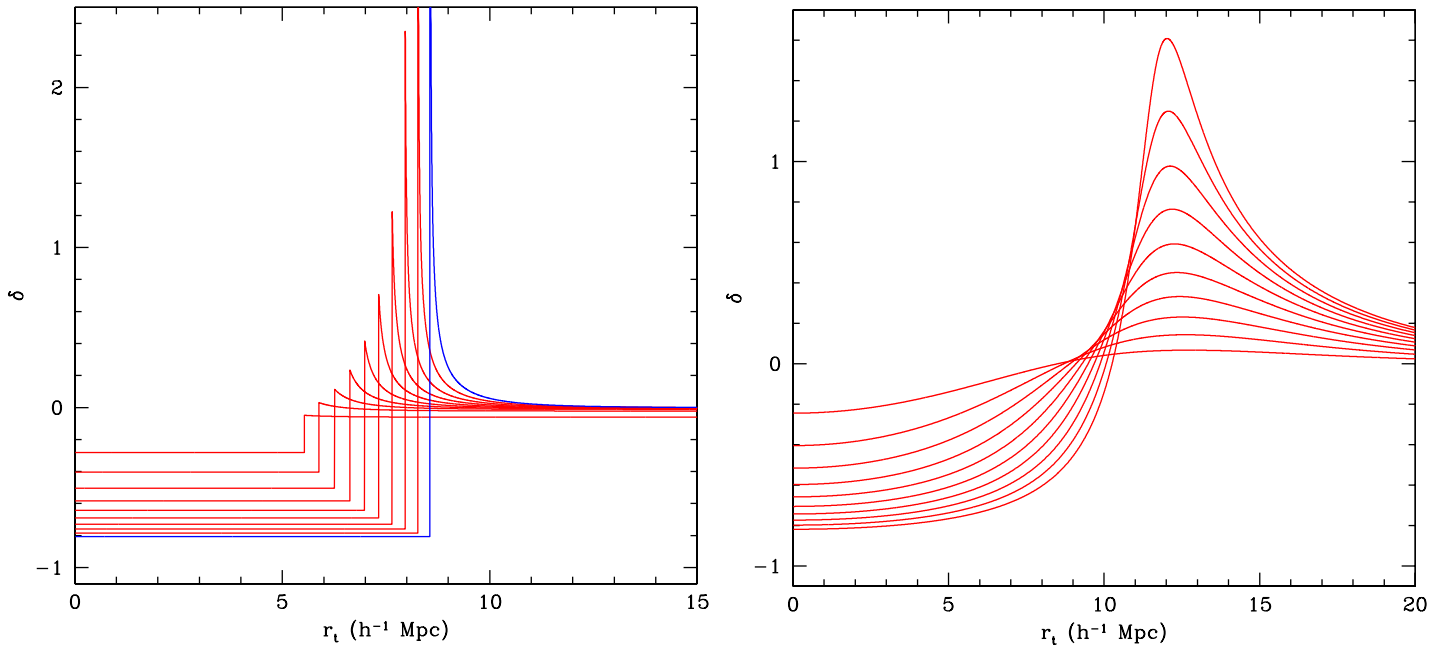

Figure 8. Spherical Voids

For a tophat void in an Einstein-de Sitter Universe the shells initially just outside the void's edge pass through a shell crossing stage at a precisely determined value of the mass shell's development angle $\Theta_r = \Theta_{sc}$,

$$\frac{\sinh\Theta_{sc}\,(\sinh\Theta_{sc} - \Theta_{sc})}{(\cosh\Theta_{sc} - 1)^2} = \frac{8}{9}, \quad \text{so } \Theta_{sc} \approx 3.53. \tag{105}$$

At this shell-crossing stage, the average density within the void is

$$1 + \Delta(r,t) \;=\; 0.1982 \tag{106}$$

times that the cosmic background density. This means that the shell has expanded by a factor of $(0.1982)^{-1/3} \approx 1.7151$. In comparison, the underdensity estimated using linear theory at the time of shell crossing is

$$\Delta_{lin}(z_{\rm sc}) = \delta_{\rm v} = -\left(\frac{3}{4}\right)^{2/3} \frac{(\sinh\Theta_{sc} - \Theta_{sc})^{2/3}}{5/3} \approx -2.81\,. \tag{107}$$

In terms of the primordial density field, the shell-crossing redshift z_{sc} of a void with (linearly extrapolated) density deficit $\Delta_{lin,0}$ may therefore be directly predicted. For an Einstein-de Sitter Universe it is

$$1 + z_{sc} \;=\; \frac{|\Delta_{lin,0}|}{2.8059}\,. \tag{108}$$

And at shell-crossing, the void has a precisely determined excess Hubble expansion rate:

$$H_s = (4/3)\,H_u(t_{sc}), \tag{109}$$

with $H_u = H_u(t_{sc})$ the global Hubble expansion factor at t_{sc}.

For a spherical underdensity, the instant of shell crossing marks a dynamical phase transition. It is as significant as the full collapse stage reached by an equivalent overdensity. Also, as with the collapse of the overdensity the timescales on which this happens are intimately related to the initial density of the perturbation. The instant of shell crossing is determined by the global density parameter Ω_i, the initial density deficit Δ_i of the shell, and the steepness of the density profile. In turn, this link between the initial void configuration and the void's *shell crossing* transition epoch paves the way towards predicting the nonlinear evolution of the cosmic void population on the basis of the primordial density field.

6. Ellipsoidal Model

Understanding the essence of the phenomenon of the formation of anisotropic patterns in the matter distribution – walls and filaments – is obtained most readily and lucidly through an assessment of an asymptotic idealization, that of the evolution of collapsing homogeneous ellipsoids. Collapsing ellipsoids tend to slow down their collapse along the longest axis while they evolve far more rapidly along the shortest axis. Starting from a near spherical configuration, the net result is a rapid contraction into a highly flattened structure as the short axis has fully collapsed. When considering the complete (homogenous) ellipsoid as a "fluid" element, the correspondence with the reasoning above is straightforward.

The bare essence of the driving mechanism behind the formation of cosmic walls and filaments is possibly best appreciated in terms of the dynamical evolution of homogenous ellipsoidal overdensities. In particular, the early work by Icke (1972, 1973) elucidated transparently the crucial characteristics of their development and morphology. On the basis of an assessment of the collapse of homogeneous ellipsoids in an expanding FRW background Universe – following the formalism of Lynden-Bell (1964) and Lin, Mestel & Shu (1965) – he came to the conclusion that flattened and elongated geometries of large scale features in the Universe should be the norm. This description intrinsically involves the self-amplifying effect of a collapsing and progressively flattening isolated ellipsoidal overdensity. Quintessential was Icke's observation that gravitational instability not only involves the runaway gravitational collapse of any cosmic overdensity, but that it has the additional basic attribute of *inevitably amplifying any slight initial asphericity during the collapse*. In order to appreciate the dynamics behind the process, and be able to assess its action within more complex situations, it is insightful to focus in some detail on the evolution of homogeneous ellipsoids.

6.0.1. *Homogeneous Ellipsoidal Model: the Formalism*

The ellipsoidal approximation involves an ellipsoidal region with a triaxially symmetric geometry, described in terms of its principal axes c_1, c_2 and c_3. The matter density in the interior of the ellipsoid has a constant value of ρ^{ell}, and the ellipsoid is embedded in a background with a density ρ_u. While the basic formalism assumes an isolated ellipsoid, we seek to extend this to a more generic configuration in which the ellipsoidal object is subjected to an external tidal field induced by matter fluctuations beyond its immediate neighbourhood. It should be noted that in principle such a configuration is a contrived one, the existence of an external field implying a *contradictio in terminis* with respect to the assumption of a homogeneous background. The intention therefore is to use this as a description reasonably approximating and illuminating relevant effects. In the presence of an this external potential contribution, the total gravitational potential $\Phi^{(tot)}(\mathbf{r})$ in the interior of a homogeneous ellipsoid is given by

$$\Phi^{(tot)}(\mathbf{r}) \;=\; \Phi_b(\mathbf{r}) \;+\Phi^{(int,ell)}(\mathbf{r}) \;+\Phi^{(ext)}(\mathbf{r}) \;, \tag{110}$$

in which (r_1, r_2, r_3) figure as the coordinates in an arbitrary Cartesian coordinate system. In this, we have decomposed the total potential $\Phi^{(tot)}(\mathbf{r})$ into three separate (quadratic) contributions,

- The potential contribution of the homogeneous background with universal density $\rho_u(t)$,

$$\Phi_b(\mathbf{r}) \;=\; \frac{2}{3}\pi G\rho_u \;(r_1^2 + r_2^2 + r_3^2) \;. \tag{111}$$

- The interior potential $\Phi^{(int,ell)}(\mathbf{r})$ of the ellipsoidal entity, superimposed onto the homogeneous background,

$$\begin{aligned} \Phi^{(int,ell)}(\mathbf{r}) \;&=\; \frac{1}{2}\sum_{m,n}\Phi^{(int,ell)}_{mn} r_m r_n \\ &=\; \frac{2}{3}\pi G(\rho^{ell} - \rho_u)\;(r_1^2 + r_2^2 + r_3^2) \;+\; \frac{1}{2}\sum_{m,n} T^{(int)}_{mn} r_m r_n \;, \end{aligned} \tag{112}$$

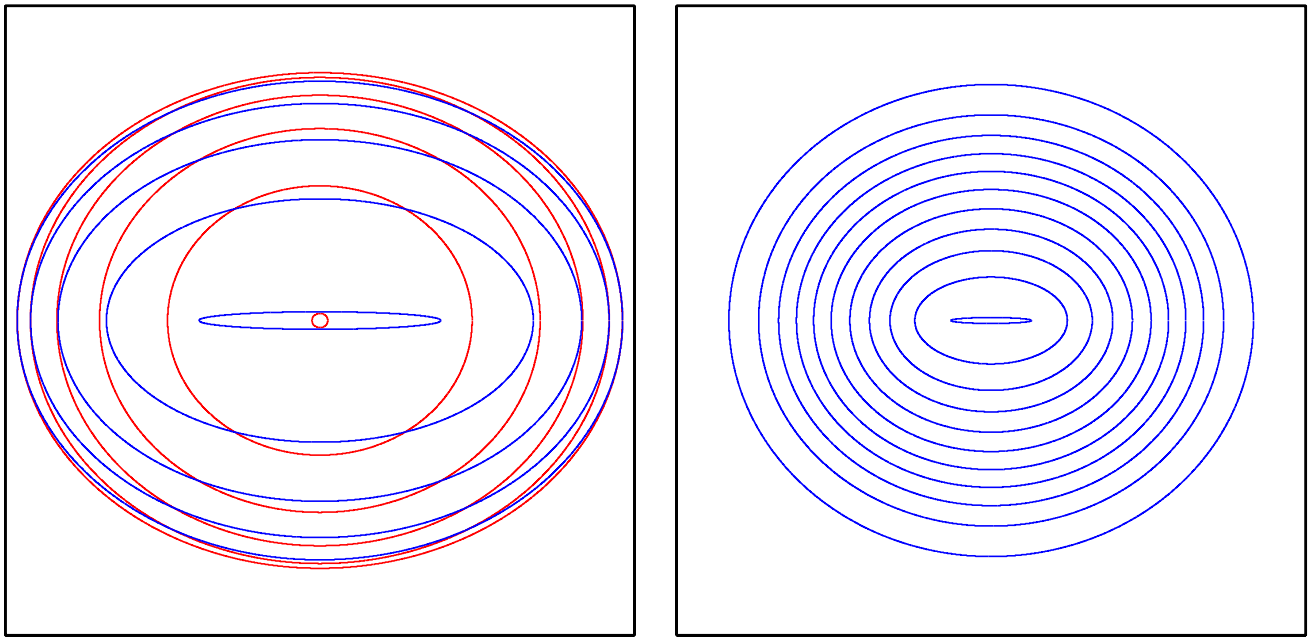

Figure 9. The evolution of an overdense homogeneous ellipsoid, with initial axis ratio $a_1 : a_2 : a_3 = 1.0 : 0.9 : 0.9$, embedded in an Einstein-de-Sitter background Universe. The two frames show a time sequel of the ellipsoidal configurations attained by the object, starting from a near-spherical shape, initially trailing the global cosmic expansion, and after reaching a maximum expansion turning around and proceeding inexorably towards ultimate collapse as a highly elongated ellipsoid. Left: the evolution depicted in physical coordinates. Red contours represent the stages of expansion, blue those of the subsequent collapse after turn-around. Right: the evolution of the same object in comoving coordinates, a monologous procession through ever more compact and more elongated configurations.

with $T^{(int)}_{mn}$ the elements of the traceless internal tidal shear tensor,

$$T^{(int)}_{mn} \equiv \frac{\partial^2\Phi^{(int,ell)}}{\partial r_m \partial r_n} - \frac{1}{3}\nabla^2\Phi^{(int,ell)}\ \delta_{mn}\ . \tag{113}$$

- The externally imposed gravitational potential $\Phi^{(ext)}$. We assume that the external tidal field not to vary greatly over the expanse of the ellipsoid, so that we can presume the tidal tensor elements to remain constant within the ellipsoidal region (cf. Dubinski & Carlberg 1991). In this approximation, the elements $T^{(ext)}_{mn}$ of the external tidal tensor correspond to the quadrupole components of the external potential field, with the latter being a quadratic function of the (proper) coordinates $\mathbf{r} = (r_1, r_2, r_3)$:

$$\Phi^{(ext)}(\mathbf{r}) = \frac{1}{2}\sum_{m,n} T^{(ext)}_{mn} r_m r_n\ . \tag{114}$$

  with the components $T^{(ext)}_{mn}$ of the external tidal shear tensor,

$$T^{(ext)}_{mn}(t) \equiv \frac{\partial^2\Phi^{(ext)}}{\partial r_m \partial r_n}\ , \tag{115}$$

  which by default, because of its nature, is a traceless tensor. Note that the quadratic form of the external potential is a necessary condition for the treatment to remain selfconsistent in terms of the ellipsoidal formalism.

As the ellipsoidal formalism does not include any self-consistent external potential, we have to impose it ourselves in an artificial way, including a specified time evolution of the tidal tensor components (see discussion in section on external tidal action, eqn. # to #), In essence, we impose an artificial external tidal field based on the assumption that the background in the immediate vicinity of the ellipsoid remains homogenous and that the external structures engendering the tidal field are located out at distances sufficiently far away from the ellipsoidal entity. This warrants the validity of the approximation by the quadratic equations, and assures that these external entities themselves are untouched themselves by the ensuing evolution of the object.

The quadratic expression for the internal ellipsoidal potential contribution $\Phi^{(int,ell)}$ can be cast into a simplified form by choosing a convenient coordinate system in which the coordinate axes coincide with the principal axes of the ellipsoid. In this case, the expression for the potential of an ellipsoid with effective density $(\rho^{ell} - \rho_u)$ and axes c_1, c_2 and c_3 reduces to (Lyttleton 1953)

$$\Phi^{(int,ell)}(\mathbf{r}) = \pi G\ (\rho^{ell} - \rho_u) \sum_m \alpha_m r_m^2\ , \tag{116}$$

where the coefficients α_m are determined by the shape of the ellipsoid,

$$\alpha_m = c_1 c_2 c_3 \int_0^\infty (c_m^2 + \lambda)^{-1} \prod_{n=1}^{3} \frac{1}{\sqrt{c_n^2 + \lambda}} \mathrm{d}\lambda\ . \tag{117}$$

As a consequence of the Poisson equation the α_m's obey the constraint: $\sum_{m=1}^{3} \alpha_m = 2$. Also, we see that the components of the internal tidal shear tensor are given by,

$$T^{(int)}_{mn} = 2\pi G(\rho^{ell} - \rho_u) \left(\alpha_m - \frac{2}{3}\right)\ \delta_{mn}\ . \tag{118}$$

It is easy to appreciate that in the case of a spherical perturbation all three α_m's are equal to 2/3, reproducing the well-known fact that in such case the internal tidal tensor contributions need to vanish.

From the quadratic nature of the total potential, the acceleration of a mass at a position $\mathbf{r}$ inside the ellipsoid, $-\nabla\Phi(\mathbf{r})$, is a linear function of $\mathbf{r}$,

$$\frac{d^2 r_m}{dt^2} \;=\; -\frac{4\pi}{3} G\rho_u r_m(t) \;-\; \sum_n \Phi^{(int,ell)}_{mn} r_n(t) \;-\; \sum_n T^{(ext)}_{mn} r_n(t) \;. \tag{119}$$

This leads to a linear relation between the location $\mathbf{r}(t) = (r_1(t),\, r_2(t), r_3(t))$ of a mass element at time t and its initial (proper) position $\mathbf{r}_i = (r_{1,i}, r_{2,i}, r_{3,i})$,

$$r_m(t) \;=\; \sum_k R_{mk}(t) r_{k,i} \tag{120}$$

in which the matrix $R_{mn}(t)$ is a spatially uniform matrix, solely dependent on time. Notice that the initial matrix $R_{mn}(t)$ is a diagonal matrix, $R_{mn}(t_i) = R_m(t_i)\delta_{mn}$. By combining Eqn. (#) and Eqn. (#), the evolution of the matrix elements R_{mk} is found to be described by

$$\frac{d^2 R_{mk}}{dt^2} \;=\; -\frac{4\pi}{3}\pi G R_{mk} \;-\; \sum_n \Phi^{(int,ell)}_{mn} R_{nk} \;-\; \sum_n T_{mn} R_{nk} \tag{121}$$

This also implies that similar points in concentric ellipsoidal shells behave in the same way, while the ellipsoid will remain homogeneous.

To appreciate the ramifications for the shape of an evolving ellipsoidal object, we exclude the torqueing and angular momentum inducing effects of the external tidal field. To this end, we make the simplifying assumption of the principal axes of the external tidal tensor to be aligned along the principal axes of the inertia tensor I_{ij} of the ellipsoid. Of course, in realistic situations we would not expect to find such a perfect alignment between the tidal and the inertia tensors. Yet, there is a significant correlation between orientation of tidal field and orientation of the principal axes of a peak/dip in a Gaussian random field. In particular, it implies a tendency to align the strongest tidal field component along the smallest axis (Van de Weygaert & Bertschinger 1996).

The principal axis alignment implies – when defining the coordinate system by the principal axes of the ellipsoid – that all off-diagonal (external) tidal tensor elements vanish, $T^{(ext)}_{mn} = T^{(ext)}_{mm}\delta_{mn}$. This implies $\sum_n T^{(ext)}_{mn} R_{nk} = T^{(ext)}_{mm} R_{mk}$. The resulting equation for the evolution of the matrix elements R_{mk} is then described by the second order diffential equation,

$$\frac{d^2 R_{mk}}{dt^2} \;=\; -2\pi G \left[\alpha_m \rho^{ell} + (\frac{2}{3} - \alpha_m)\; \rho_u \right] R_{mk} \;-\; T^{(ext)}_{mm} R_{mk} \;. \tag{122}$$

Evidently, the coupling between the different components R_{mk} vanishes. As they are initially equal to zero this implies the non-diagonal elements $R_{mk}(t)$ to remain so, $R_{mk}(t) = R_m(t)\delta_{mn}$. At time t, a mass element initially at (proper) position $\mathbf{r}_i = (r_{1,i}, r_{2,i}, r_{3,i})$ has therefore moved to position $\mathbf{r}(t) = (r_1(t), r_2(t), r_3(t)) = (R_1(t)r_{1,i}, R_2(t)r_{2,i}, R_3(t)r_{3,i})$, in which the functions $R_m(t)$ evolve according to

$$\frac{d^2 R_m}{dt^2} \;=\; -2\pi G \left[\alpha_m \rho^{ell} + (\frac{2}{3} - \alpha_m)\; \rho_u \right] R_m \;-\; T^{(ext)}_{mm} R_m \;. \tag{123}$$

The evolution of the ellipsoid is thus fully encapsulated in terms of the the functions $R_1(t)$, $R_2(t)$ and $R_3(t)$, which in essence should be seen as scale factors of the principal axes of the ellipsoid,

$$c_m(t) \;=\; R_m(t) c_{m,i} \;. \tag{124}$$

For any initial configuration of a homogeneous ellipsoid embedded in a FRW background Universe with current cosmic density parameter $\Omega_\circ$ and Hubble parameter $H_\circ$, specified by its initial characteristics at cosmic expansion factor a_i,

- The initial principal axes, (c_1, c_2, c_3).

- The initial ellipsoidal density ρ_i^{ell}, in terms of density contrast δ_i

$$\delta_i \equiv \frac{\rho_i^{ell} - \rho_{ui}}{\rho_{ui}} , \tag{125}$$

with respect to the background Universe with initial cosmic density

$$\rho_{ui} = \frac{3}{2}\,\Omega_\circ H_\circ \left(\frac{a_\circ}{a_i}\right)^3 \tag{126}$$

the evolution of the scale factors $R_m(t)$ can be fully recovered once the boundary conditions have been set, i.e.

- The initial scale factors,

$$R_m(t_i) = 1 \tag{127}$$

for $(m = 1, 2, 3)$.

- The initial velocity perturbation,

$$\begin{aligned} v_m(t_i) = (dR_m/dt)\, r_{m,i} &= v_{Hubble,m}(t_i) + v_{pec,m}(t_i) \\ &= H_i\, R_m r_{m,i} + v_{pec,m}(t_i) , \end{aligned} \tag{128}$$

for $(m = 1, 2, 3)$, which when choosing to follow the growing mode solution of linear perturbation theory (Peebles 1980) is given by

$$\begin{aligned} v_{pec,m}(t_i) &= \frac{2f(\Omega_i)}{3H_i\Omega_i} g_{pec,m}(t_i) \\ &= -\frac{1}{2} H_i f(\Omega_i) \left[\alpha_{m,i}\delta_i + \frac{4T^{(ext)}_{mm,\circ}}{3\Omega_0 H_0^2}\, D_i\right] r_{m,i} . \end{aligned} \tag{129}$$

In the latter expression, $f(\Omega_i)$ is the corresponding linear velocity growth factor (Peebles 1980). The $\alpha_{m,i}$ are the values of the ellipsoidal shape factors α_m at expansion factor, which are yielded after evaluating the integral expression (#) for the specified initial axis ratios. For this expression, we specified the (artificially imposed) time development of the external tidal tensor through a growth factor $D(t)$, $E_{mm}/\Omega H^2 \propto D(t)$, relating the current external tidal field $T^{(ext)}_{mm,\circ}$ to its initial value.

6.0.2. *Homogeneous Ellipsoidal Model: the Approximation*

Evidently, we have to be aware of the serious limitations of the ellipsoidal model. It grossly oversimplifies in disregarding important aspects like the presence of substructure in and the immediate vicinity of peaks and dips in the primordial density field, the sites it typically deals with. Even more serious is its neglect of any external influence, whether the secondary infall or "collision" with surrounding matter or the role of nonlocal tidal field engendered by the external mass distribution. For overdensities it represents a reasonable approximation for moderately evolved features like a Megaparsec (proto)supercluster, but it will be seriously flawed in the case of highly collapsed objects like galaxies and even clusters of galaxies. Nonethelss, the concept of homogeneous ellipsoids has proven to be particularly useful when seeking to develop approximate yet advanced descriptions of the distribution of virialized cosmological objects (Bond & Myers 1996a,b,c, and Sheth, Mo & Tormen 2001).

Interestingly, in many respects the homogeneous model is a better approximation for underdense regions than it is for overdense ones. Overdense regions contract into more compact and hence steeper

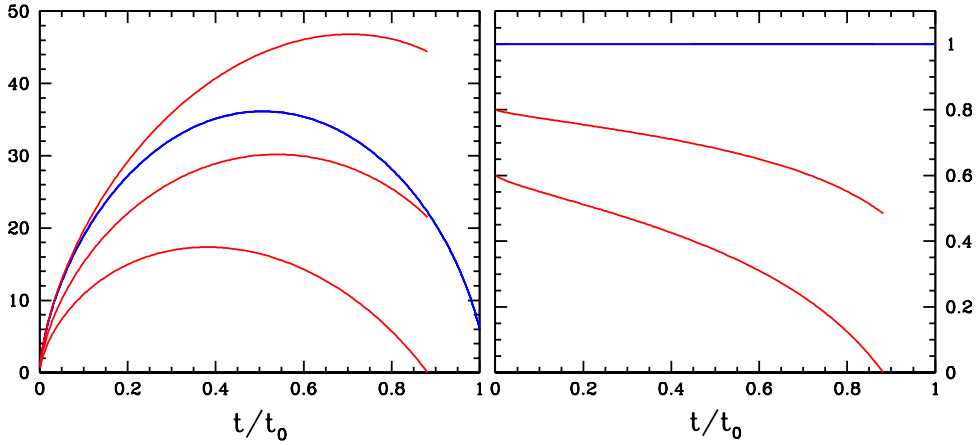

Figure 10. The evolution of an overdense homogeneous ellipsoid, with initial axis ratio $a_1 : a_2 : a_3 = 1.0 : 0.8 : 0.6$, in an Einstein-de-Sitter background Universe. Left: expansion factors for each individual axis; right: axis ratios a_2/a_1 and a_3/a_1. The ellipsoid axes are depicted as red curves. For comparison, in blue, the evolution of an equivalent homogenous spherical overdensity.

density peaks, so that the area in which the ellipsoidal model represents a reasonable approximation will continuously shrink. On the other hand, while voids expand and get drained, the density fields in the central region of the (proto)void will flatten out, so that the voids develop into regions of a nearly uniform density and the region of validity of the approximation grows accordingly. This can be readily appreciated from the conceptually simpler spherical model approximation. More significant, it was also demonstrated in the complex circumstances of voids embedded in a general cosmic density field for a set of N-body structure formation simulations (Van de Weygaert & van Kampen 1993, see Fig. #). A direct repercussion of the flattening out of the voids is the velocity field inside them. With the exception of the ridges surrounding them, the quadratic potential approximation will be valid for most of the void's interior and therefore be characterized by a velocity field of excess Hubble expansion. The systematic study by Van de Weygaert & Van Kampen (1993) indicated how the void velocity fields in general will evolve towards a state in which they become genuine "Superhubble Bubbles" (see section #). Evidently, the ellipsoidal approximation will only be useful for the interior of voids. At the outer fringes the neglect of the role of surrounding material will be rendered invalid, as the sweeping up of matter, the formation and subsequent induced 'self-interaction' and the encounter with surrounding structures will become domineering effects.

7. N-body simulations

With the exception of a few attempts towards an Eulerian implementation (e.g. Peebles 1987), efforts which gradually gain more ground with the inclusion of gas-dynamical and radiative processes, computational efforts have concerned N-body computer simulations. By nature, this involves a translation of the evolution of a system into a Lagrangian formulation, in which the computer gets instructed to follow the path of each particle into which the initial density field had been broken up. Fully nonlinear N-body computer simulations have produced the most readily visible, and directly appealing and accessible, descriptions of the way into which the gravitational instability process manages to mould the primordial universe into rich structural patterns.

Truely giant technological advances over the past decades have provided us with a comprehensive, physically justified and badly needed visual impression of the way into which the mutual influence of the combined gravitational forces unleashed by the matter perturbations throughout the cosmos works its way towards the emergence of structure. It has allowed the recognition of some basic mechanisms during the full nonlinear evolution of self-gravitating systems. The spatial patterns in the resulting particle distributions, as well as their kinematics and dynamics, provide us with an excellent testbed for testing and comparing quantitatively a large range of viable structure formation scenarios. However, they suffer

from a variety of restricting effects, and we should be anxious not to overinterpret and/or overestimate the results of their performance.

Firstly, they can only go as far as allowed by the physics implemented into them. They will and cannot reveal basic new science to us. The full array of relevant physics, in particular when we get below scales of clusters of galaxies, is not confined to merely gravitational influences. Radiative processes, a complex interplay of various hydrodynamic processes, star formation processes, and the full impact of involved feedback interactions should make us realize the limitations of the outcome of the calculations. A large industry of new complex computer codes attempt to deal with at least a selection of these influences. They, however, also illustrate the daunting and possible unsurmountable challenges awaiting us in formulating a fully and uniquely defined scenario of structure formation, incorporating every necessary aspect of relevant physics.

Even when restricting ourselves to purely gravitational systems, strictly only applicable to scales at which nongravitational dissipation can be fully discarded as irrelevant, their results should still be considered as merely approximate and indicative. Their dynamic range is usually very limited. This is true for the feasible spatial resolution, for the attainable mass resolution, as well as for the range of timescales that can be covered by them. As available computer memory will always restrict these, the full spatial range of fluctuations – even influential ones – can never be properly represented within a given cosmic region. A representation of the full primordial power spectrum of density fluctuations is beyond the grasp of any conceivable piece of equipment. It is therefore important that claims of validity of specific formation scenarios can never be fully justified. In addition, the limited dynamic range will also restrict the force resolution during the nonlinear evolution, which is particularly cumbersome on the smallest scales which produce the first nonlinear entities. In addition, we see a rapid increase in computational expense as we try to improve the resolution. Even though the availability of ultrafast computing machinery with ever growing huge memory capacity has expanded the achievements of cosmological N-body computer simulations to truely dramatic levels, the demands grow along with them, a pace not necessarily followed equally fast by the insights going along with them.

An additional restriction for N-body codes is that they can strictly only be applied to initial value problems (see section 3.5.3). For pure theoretical purposes, this does not pose a restriction. For a given cosmological and structure formation model the initial density and velocity field are specified and subsequently evolved and analyzed. However, when turning to the observed world, we may recognize that we are usually dealing with analyzing situations in which most information is available for the present epoch. In most cases this involves nonlinear structures for which we are not able to extrapolate in a straightforward and direct fashion towards the initial conditions. Hence we are unable to use N-body techniques towards analyzing the implications for the dynamics and evolution of the observed structures.

Possibly the most important limitation of computer calculations may be that the understanding of the dynamics and physics of the simulated systems is not significantly increased. *Simulations will not increase our understanding of dynamics without guidance from analytical approaches*, and therefore analytical approximations will be absolutely essential for that purpose. Along one direction, these do provide us with a handle to interpret the outcome of the computer experiments. Equally important, they direct us in defining the best possible computer models and configurations.

Even more important it is to be aware that full understanding involves the formulation of analytical descriptions, which should embody our insights into the systematics and regularities of a system, the true purpose of scientific inquiry. Analytical descriptions should therefore be the preferred endgoal, the computer experiments, along with the ever growing body of available observations, are there to guide and sharpen our insight and intuition.